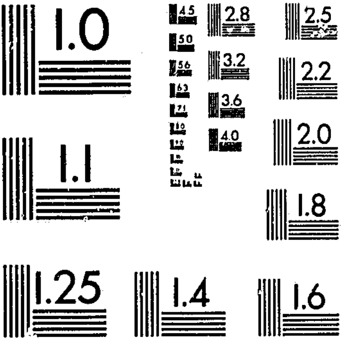

MICROCOPY RESOLUTION TEST CHART
NATIONAL BUREAU OF STANDARDS
STANDARD REFERENCE MATERIAL 1010a
(ANSI and ISO TEST CHART No. 2)

PSU/TURBO 83-1

SEMI-ANNUAL PROGRESS REPORT ON
THREE DIMENSIONAL FLOW FIELD INSIDE COMPRESSOR ROTOR, INCLUDING BLADE BOUNDARY LAYERS

M. POUAGARE, B. LAKSHMINARAYANA, & J. M. GALMES

(NASA-CR-169788) THREE DIMENSIONAL FLOW FIELD INSIDE COMPRESSOR ROTOR, INCLUDING BLADE BOUNDARY LAYERS Semiannual Progress Report (Pennsylvania State Univ.) 52 p HC A04/MF A01 CSCL 20A G3/34
N83-16679
Unclas
08411

NASA GRANT NSG 3266
NATIONAL AERONAUTICS & SPACE ADMINISTRATION
LEWIS RESEARCH CENTER

TURBOMACHINERY LABORATORY
DEPARTMENT OF AEROSPACE ENGINEERING
THE PENNSYLVANIA STATE UNIVERSITY
UNIVERSITY PARK, PA 16802

JANUARY 1983

4. COMPOSITE THREE-DIMENSIONAL PROFILES OF THE VELOCITY AND PRESSURE FIELD IN THE A.F.C. ROTOR

The flow field in the AFC rotor can be divided into different regions (inviscid core region, end-wall region, tip-leakage, blade boundary layer). Different types of probes were used to measure the various regions. The type of probe used at each region is dictated by the flow field characteristics of that region (three or two dimensional, high or low turbulent). Four different sets of measurements were performed in the PSU/TURBO AFC rotor. The core inviscid flow was measured with a rotating five hole probe, the end-wall region with a rotating three sensor hot wire, the blade boundary layer with a rotating two sensor hot wire and the tip leakage flow with a stationary two sensor hot wire.

We are now in the process of combining all these data together in order to acquire a complete picture of the flow field in the rotor. Some of the completed composite profiles are shown in Figs. 16 through 20.

Figure 16 shows the relative streamwise velocity Q_S plotted versus the tangential and radial directions at the streamwise location S = 0.979. This figure combines the blade boundary layer data, the inviscid core data and the end-wall data. In Fig. 17 the tip-leakage data are also included. As expected the relative velocity Q_S goes to one near the casing.

Figure 18 shows the radial velocity (Q_R) plotted versus the axial and tangential distance at R = 0.973. A strong inward radial velocity can be clearly seen at the mid-passage. This is because of the tip leakage. In this figure only the end-wall data are shown.

PSU-Turbo-83-1

Semi-Annual Progress Report

on

THREE DIMENSIONAL FLOW FIELD INSIDE COMPRESSOR ROTOR PASSAGES, INCLUDING BLADE BOUNDARY LAYERS

M. Pouagare, B. Lakshminarayana and J. M. Galmes

to

NASA Lewis Research Center

Project Monitor: Dr. P. Sockol

Turbomachinery Laboratory
Department of Aerospace Engineering
The Pennsylvania State University
University Park, PA 16802

January 1983

PREFACE

The progress of research on "Three Dimensional Flow Field Inside a Compressor Rotor Blade Passage, Including Blade Boundary Layers" (NASA Grant NSG 3266) for the six-month period ending December 31, 1982, is briefly reported here. The effort on turbulence modelling is incorporated into the paper "A Turbulence Model for Three Dimensional Turbulent Shear Flow Over Curved Rotating Bodies," AIAA Paper No. 83-0559. A copy of this paper was transmitted to NASA recently. For the sake of brevity, the material in this paper will not be repeated here.

B. Lakshminarayana
Principal Investigator

TABLE OF CONTENTS

Page

NOMENCLATURE FOR CHAPTER I iv

NOMENCLATURE FOR CHAPTERS 3 AND 4 v

1. NUMERICAL SOLUTION OF THE FLOW FIELD INSIDE THE PASSAGE OF A TURBOMACHINERY ROTOR PASSAGE 1

   Modification of the Equations 1
   Turbulence Modeling 2
      Status of the Code 3

2. A TURBULENCE MODEL FOR THREE DIMENSIONAL TURBULENT SHEAR FLOW OVER CURVED ROTATING BODIES 4

3. BLADE BOUNDARY LAYER IN AN AXIAL FLOW COMPRESSOR ROTOR . . 5

   Measurement Technique and Corrections for Wall Vicinity Effect 5
   Correction for Spatial Error 7
   Experimental Results 7

4. COMPOSITE THREE-DIMENSIONAL PROFILES OF THE VELOCITY AND PRESSURE FIELD IN THE A.F.C. ROTOR 9

PUBLICATIONS & PRESENTATIONS 12

REFERENCES 13

APPENDIX A 14

FIGURES 27

NOMENCLATURE FOR CHAPTER 1

J	Jacobian of the transformation
P	Pressure
r,θ,z	cylindrical coordinate system
U,V,W	velocities in axial, tangential, and radial direction, respectively
n_z, n_θ, n_r	$\frac{\partial n}{\partial z}, \frac{\partial n}{r\partial\theta}, \frac{\partial n}{\partial r}$
R_z, R_θ, R_r	$\frac{\partial R}{\partial z}, \frac{\partial R}{r\partial\theta}, \frac{\partial R}{\partial r}$
ξ_z, ξ_θ, ξ_r	$\frac{\partial \xi}{\partial z}, \frac{\partial \xi}{r\partial\theta}, \frac{\partial \xi}{\partial r}$
μ	molecular viscosity
ξ, n, R	transformed coordinates in the streamwise, normal and radial directions, respectively
ρ	density
Ω	angular velocity
k	turbulent kinetic energy
ε	turbulent dissipation rate
Re	Reynolds number
u^*	friction velocity
Q_p	resultant velocity parallel to the wall at the first grid point away from the wall
e_i	internal energy

$u = \xi_z U + \xi_\theta V + \xi_r W$

$v = n_z U + n_\theta V + n_r W$

$w = R_z U + R_\theta V + R_r W$

ν	kinematic viscosity

Subscripts

p	value of the first grid point away from the wall

NOMENCLATURE FOR CHAPTERS 3 and 4

C	chord length
ℓ,d	length and diameter of the hot wire
N	n/C
R	r/r_{tip}
S	s/C
PS,SS	pressure and suction surface, respectively
s,n,r	streamwise, normal, and radial directions (orthogonal to each other) shown in Fig. 1. s = 0 at the leading edge, n = 0 on the blade surface, r = 0 at the axis of the machine.
U	streamwise relative velocity normalized by U_e
U_e	local free stream (or edge) relative velocity
W	the difference between the local radial velocity and the free stream radial velocity normalized by U_e.
T_{se}	the free stream value of the streamwise relative intensity normalized by U_e.
T_{re}	the free stream value of the radial intensity normalized by U_e.
T_s	relative streamwise intensity normalized by T_{se}
T_r	radial intensity normalized by T_{re}
Q_S	relative streamwise velocity in the s-n plane normalized by the blade tip speed
Q_R	radial velocity normalized by the blade tip speed
Y	tangential distance normalized by the spacing and measured from the blade surface (Y = 0 on the suction side, Y = 1 on the pressure side).
P_S	static pressure normalized by $\frac{1}{2}\rho U_t^2$
P_T	total pressure normalized by $\frac{1}{2}\rho U_t^2$
U_t	blade tip speed

I. NUMERICAL SOLUTION OF THE FLOW FIELD INSIDE THE PASSAGE OF A TURBOMACHINERY ROTOR PASSAGE

The space marching code, developed by Govindan and Lakshminarayana [1], has been modified in order to be able to predict the flow field inside a rotor passage, including the blade and hub wall boundary layers. The basic changes incorporated are as follows:

(i) Modifications of the equations so that the code can handle three-dimensional configurations with changes in the radial direction (for example changes in stagger angle, blade camber and thickness.

(ii) Extensions and modifications in order to implement physically realistic turbulence model such as k-ε model and algebraic Reynolds stress model

1.1 Modification of the Equations

The equations in the original code are based on the transformation of the compressible flow equation from a cylindrical coordinate system (r,θ,z) to a body fitted coordinate system (R,ξ,n) through the transformation

$$\xi = \xi(z,\theta)$$
$$n = n(z,\theta) \qquad (1)$$
$$R = R(r)$$

for the code to handle fully three dimensional geometries the transformation should be

$$\xi = \xi(r,\theta,z)$$
$$n = n(r,\theta,z) \qquad (2)$$
$$R = R(r,\theta,z)$$

The equations and the corresponding Jacobian matrices have been derived in the body fitted coordinates given by Eq. (2). The results are given in Appendix A.

1.2 Turbulence Modeling

The algebraic Reynolds stress model developed in Ref. 2 and the k-ε model described in Ref. 3 have been coded and integrated with the main space marching code.

The calculation of the turbulent kinetic energy, dissipation and Reynolds stresses are lagged one streamwise step. The five equations (continuity, three momentum, and energy) are first solved using the turbulence quantities derived at the previous streamwise step. When ρ, U, V, W, e_i are calculated, the k and ε equations are solved in order to derive the values of k and ε. The algebraic system of equations for the Reynolds stresses is then invert ' to derive the Reynolds stresses. These stresses are used in the next streamwise station.

In order to avoid using a very large number of grid points near the walls, the so-called wall-functions are used [4]. This approach assumes that, at the first grid point away from the wall with wall distance n_p just outside the viscous sublayer, the velocity components parallel to the wall follow the logarithmic law of the wall and the turbulence is in local equilibrium. With these assumptions, the resultant velocity parallel to the wall Q_p, the kinetic energy k_p and the dissipation rate ε_p at point n_p are related by the following relationships

ORIGINAL PAGE IS
OF POOR QUALITY

$$\frac{Q_p}{u^*} = \frac{1}{k} \ln \left(E \frac{u_* n_p}{\nu} \right), \quad k_p = \frac{u^{*3}}{\sqrt{C_\mu}}, \quad \varepsilon_p = \frac{u^{*3}}{KY_p}$$

where K, E, C_μ are constants; K = 0.4, E = 9, C_μ = 0.09

1.2.1 Status of the code The subroutines implementing the k-ε model and the Reynolds stress model have been completed and integrated with the main code. The code is presently tested in simple turbulent flow configurations for debugging purposes.

2. A TURBULENCE MODEL FOR THREE DIMENSIONAL TURBULENT SHEAR FLOW OVER CURVED ROTATING BODIES

It is known that the curvature and rotation affect the turbulence structure substantially and a knowledge of these effects are essential for the improved prediction of flow over rotating bodies. A turbulence model which includes the effects of curvature as well as rotation was developed during this reporting period. For the sake of brevity, this analysis is not presented in this report as it has been published as an AIAA Paper, "A Turbulence Model for Three Dimensional Shear Flow Over Curved Rotating Bodies," J. Galmes and B. Lakshminarayana, AIAA Paper No. 83-0559. Different hypotheses introduced to model the higher order unknowns in the Reynolds stress equations are presented in this paper; a set of algebraic equations is derived. The transport equations of the turbulent kinetic energy and dissipation rate are discussed. A detailed analysis of the effect of the rotation on each component of the Reynolds stress tensor is presented for hypothetical cases such as the pure shear flow in a rotating frame. Calculations show that the effects of rotation on turbulent shear stresses are more pronounced in a centrifugal type of turbomachinery than an axial type.

3. BLADE BOUNDARY LAYER IN AN AXIAL FLOW COMPRESSOR ROTOR

The three-dimensional turbulent boundary layer developing on the rotor of the compressor of the PSU/TURBO Lab was measured using a miniature "x" configuration hot wire probe. This investigation started earlier and its major part was completed in the period July - December 1982. The measurements were carried out at nine radial locations on both surfaces of the blade at various chordwise locations (see Table 1).

3.1 Measurement Technique and Corrections for Wall Vicinity Effect

All the velocity and turbulence measurements were taken with a miniature crossflow "x" wire probe TSI (1247) shown as an insert in Fig. 2. The sensors were 3 mm diameter platinum-tungsten wires with $\ell/d \approx 300$. The sensors were located in the (sr) plane with their axis at 45° to the s axis (Fig. 1) and were traversed normal to the blade surface. Since the flow traverse was done close to the blade surface, the component of velocity in the n direction (V) is assumed to be small. The present configuration together with the relevant hot wire equations [5] provide the value of the streamwise velocity U, radial velocity W and the respective intensities T_s and T_r in the s,n,r system shown in Fig. 1. The s coordinate is parallel to the blade surface lying on the cylindrical plane, n is the principal normal and r is the radial direction as shown in Fig. 1. The coordinate system is orthogonal.

Since the measurements were taken very close to the blade surface and the heat transfer characteristics are affected by the wall vicinity, the hot wire probe was calibrated to derive corrections for the wall vicinity effect. These are incorporated into the hot wire equations of Ref. 5. The probe was calibrated in a jet with a wall (parallel to the jet) at the exit. The distance between the wall and the probe continuously varied from 0.05 mm to 5 mm, beyond which the change in calibration curve was found to be negligibly small. The calibration curve is shown in Fig. 2. The data includes the voltage at zero velocity (E_o) as well as the voltage (E) at various jet velocities (Q). It is clear from Fig. 2 that the exponent in King's law is not affected by the wall. King's law is given by

$$E^2 - E_o^2 = BQ^n \tag{3}$$

where B is a calibration constant and n is the exponent. The values of E_o and B are affected by the wall vicinity. The correlation for the wall vicinity based on this data is given by,

$$E_c^2 = (E_{o\infty}^2 - E_{ow}^2) \frac{D}{D_\infty} + E_{ow}^2. \tag{4}$$

where $E_{o\infty}$ is the value of E_o at $D = D_\infty$, and E_{ow} is the voltage at zero velocity near the wall. D is the distance between the sensor nearest to the wall and the wall. The value of D_∞ = 5 mm and D = 0.05 mm, 1.25 mm, 2.5 mm, and 5 mm. The shift in the data shows that the coefficient B is affected and the following correlation for B is derived from this data.

$$B = C B_\infty \exp\left(- \frac{D}{D_\infty} \log C\right), \quad C = 1.01$$

where B_∞ is the coefficient away from the wall.

It appears that without the corrections introduced through Eqs. (4) and (5) there is an error of approximately 6 percent in the velocity close to the wall. These corrections (Eqs. (4) and (5)) have been incorporated in the hot wire equations. The value of E_{ow} and E_{o_∞} were measured at the beginning and the end of each measurement run.

3.2 Correction for Spatial Error

The two sensors of the probe are not exactly at the same location but are spaced at 0.51 mm apart. In order to correct the error introduced by this distance, the velocity that each wire feels (V_1,V_2) is plotted separately versus the true distance of each wire (N_1,N_2) from the wall (Fig. 3). Then the streamwise and radial velocity components at some distance N_1 (the distance of the closest to the wall wire) are calculated using the value of V_1 at N_1 and the interpolation (or extrapolated) values of V_2 at the location N_1. Figure 4 shows both the corrected and uncorrected values of U and W for the measured boundary layers on the suction side of the blade at R = 0.75. All the subsequent figures show the corrected values of U and W. The turbulence intensities cannot be corrected for the spatial error. Judging from the mean velocites (Fig. 4) the correction is not large and it is confined only to a few points near the wall.

3.3 Experimental Results

Results at selected radial locations, R = 0.75, 0.918, 0.98, are given. The complete set of data will be included in a report under preparation.

Figures 4 through 6 show the boundary layer development on the suction side of the blade at the three radial locations. Figures 7 through 9 show the corresponding results on the pressure side of the blade. It can be clearly seen that at the trailing edge region the boundary layer thickness is approximately two times larger on the suction side than on the pressure side. Going from lower to higher radii the boundary layer thickness is increasing on the suction side and stays approximately constant on the pressure side. In the end-wall region ($R = 0.918$ to $R = 0.98$), the effect of tip leakage which acts as a "suction" on the boundary layer on the pressure side and as a "blowing" on the suction side can be seen.

The radial velocity is outwards at most locations. On the suction side it is decreasing towards the top while on the pressure side it is increasing. This again can be attributed to the tip leakage effects.

Figures 10 through 15 show the turbulent quantities at the three radial locations on the suction and pressure sides of the blade. The turbulent intensities T_s, T_r are normalized respectively by the free stream turbulent intensities T_{se}, T_{re}. It is interesting to note that T_r and T_s have almost the same values at all locations. For a stationary boundary layer $T_s > T_r$. The reason that $T_s \approx T_r$ is probably due to the rotation effect, analyzed in Ref. 6.

Figures 19 and 20 show, respectively, the static pressure P_S and tht total pressure P_T plotted versus the radial and tangential directions. P_S is at the streamwise location S = 0.25 and P_T is at S = 0.979. In the last two figures only the inviscid core data are shown.

Table 1

Radial and Streamwise Measurement Locations
of the Blade Boundary Layer

R	Pressure Side Distance S				Suction Side Distance S			
0.583	0.22	0.44	0.68	0.92	0.49	0.66	0.81	0.99
0.67	0.23	0.48	0.70	0.93	0.55	0.69	0.84	0.99
0.75	0.24	0.52	0.73	0.94	0.60	0.72	0.87	0.99
0.823	0.245	0.525	0.75	0.95	0.63	0.77	0.9	0.99
0.918	0.25	0.53	0.76	0.96	0.65	0.81	0.94	0.99
0.945	0.26	0.54	0.78	0.97	0.66	0.83	0.96	
0.959	0.265	0.545	0.785	0.975	0.665	0.835	0.97	
0.973	0.27	0.55	0.79	0.98	0.67	0.84	0.98	
0.98	0.27	0.55	0.79	0.98	0.67	0.84	0.99	

PUBLICATIONS & PRESENTATIONS

The following papers were published during this period:

(1) B. Lakshminarayana, T. R. Govindan, and C. Hah, "Experimental Study of the Boundary Layer on a Turbomachinery Rotor Blade." In Three Dimensional Turbulent Boundary Layers, edited by H. H. Fernholz and E. Krause, IUTAM Symposium Proceedings; Springer-Verlag, pp. 165-176.

The following presentations were made during the reporting period:

(1) "Computation Measurement of Rotor Wake Including Turbulence Modelling," William Maxwell Reed Mechanical Engineering Seminar, University of Kentucky, September 23, 1982.

(2) "Turbulence Modelling and Turbomachinery Flow Computation," Workshop on Trubomachinery Flow Computation, NASA Lewis Reserach Center, October 21, 1982.

REFERENCES

1. Govindan, T. R., Lakshminarayana, B., and Murthy, K. N. S., "Endwall Flows in Rotors and Stators of a Single Stage Compressor," Semi-Annual Progress Report on NASA Grant NSG 3212, June 1982.

2. Galmes, J. M., Pouagare, M., and Lakshminarayana, B., "Semi-Annual Progress Report on Three Dimensional Flow Field Inside Compressor Rotor Passages, Including Blade Boundary Layers," NASA Grant NSG 3266, July 1982.

3. Lakshminarayana, B., "Three Dimensional Flow Field Inside Compressor Rotor Passages, Including Blade Boundary Layers," A proposal for the continuation of the NASA Grant NSG 3266.

4. Rodi, W., "Examples of Turbulence Models for Incompressible Flows," AIAA Journal, Vol. 20, 1981, pp. 872-879.

5. Klatt, F., "The X Hot-Wire Probe in a Plane Flow Field," DISA Information No. 8, July 1969.

6. Galmes, J. M., Lakshminarayana, B., "An Algebraic Reynolds Stress Model for Three-Dimensional Turbulent Shear Flows Over Curved Rotating Bodies," AIAA paper 83-0559 (copy is enclosed).

APPENDIX A

The continuity, the three momentum and the energy equations are written in the form

$$\frac{\partial E}{\partial \xi} + \frac{\partial F}{\partial n} + \frac{\partial G}{\partial R} + C = \frac{1}{Re}\left[\frac{\partial P}{\partial R} + \frac{\partial Q}{\partial n} + S\right].$$

E, F, G, C, P, Q, S are 5x1 column vectors and are given below:

$$E = \frac{1}{J}\begin{bmatrix} \rho u \\ \rho u U + \xi_z P \\ \rho u V + \xi_\theta P \\ \rho u W + \xi_r P \\ \rho u\left(\gamma e_i + \frac{U^2+V^2+W^2}{2}\right) \end{bmatrix} \qquad F = \frac{1}{J}\begin{bmatrix} \rho v \\ \rho v U + n_z P \\ \rho v V + n_\theta P \\ \rho v W + n_r P \\ \rho v\left(\gamma e_i + \frac{U^2+V^2+W^2}{2}\right) \end{bmatrix}$$

$$G = \frac{1}{J}\begin{bmatrix} \rho w \\ \rho w U + R_z P \\ \rho w V + R_\theta P \\ \rho w W + R_r P \\ \rho w\left(\gamma e_i + \frac{U^2+V^2+W^2}{2}\right) \end{bmatrix} \qquad C = \begin{bmatrix} W/R \\ \rho \frac{UW}{R} \\ \frac{2\rho VW}{R} + 2\rho\Omega W \\ \rho \frac{(W^2-V^2)}{R} - \rho\Omega^2 R - 2\rho\Omega V \\ \frac{W}{R}(\gamma\rho e_i) + \rho\frac{U^2+V^2+W^2}{2} - \rho\Omega^2 RW \end{bmatrix}$$

$$P_1 = 0$$

$$P_2 = \frac{\mu}{J}\Big[(R_r^2 + R_\theta^2 + \tfrac{4}{3}R_z^2)\frac{\partial U}{\partial R} + \frac{R_\theta R_z}{3}\frac{\partial V}{\partial R} + \frac{R_r R_z}{3}\frac{\partial W}{\partial R} + (R_r n_r + R_\theta n_\theta + \tfrac{4}{3}n_z R_z)\frac{\partial U}{\partial n}$$
$$+ (R_\theta n_z - \tfrac{2}{3}R_z n_\theta)\frac{\partial V}{\partial n} + (R_r n_z - \tfrac{2}{3}R_z n_r)\frac{\partial W}{\partial n} - \tfrac{2}{3}R_z\frac{W}{R}\Big]$$

$$P_3 = \frac{\mu}{J}\left[\frac{R_\theta R_z}{3}\frac{\partial U}{\partial R} + (R_r^2 + \frac{4}{3}R_\theta^2 + R_z^2)\frac{\partial V}{\partial R} + \frac{R_r R_\theta}{3}\frac{\partial W}{\partial R} + (n_\theta R_z - \frac{2}{3}R_\theta n_z)\frac{\partial U}{\partial n}\right.$$

$$\left. + (R_r n_r + \frac{4}{3}R_\theta n_\theta + R_z n_z)\frac{\partial V}{\partial n} + (R_r n_\theta - \frac{2}{3}R_\theta n_r)\frac{\partial W}{\partial n} - R_r\frac{V}{R} + \frac{4}{3}R_\theta\frac{W}{R}\right]$$

$$P_4 = \frac{\mu}{J}\left[\frac{R_r R_z}{3}\frac{\partial U}{\partial R} + \frac{R_r R_\theta}{3}\frac{\partial V}{\partial R} + (\frac{4}{3}R_r^2 + R_\theta^2 + R_z^2)\frac{\partial W}{\partial R} + (R_z n_r - \frac{2}{3}R_r n_z)\frac{\partial U}{\partial n}\right.$$

$$\left. + (R_\theta n_r - \frac{2}{3}R_r n_\theta)\frac{\partial V}{\partial n} + (\frac{4}{3}R_r n_r + R_\theta n_\theta + R_z n_z)\frac{\partial W}{\partial n} - \frac{2}{3}R_r\frac{W}{R} - R_\theta\frac{V}{R}\right]$$

$$P_5 = \frac{\mu}{J}\left[\frac{\partial U}{\partial n}\left(U(n_r R_r + n_\theta R_\theta + \frac{4}{3}n_z R_z) + V(R_z n_\theta - \frac{2}{3}R_\theta n_z) + W(R_z n_r - \frac{2}{3}R_r n_z)\right)\right.$$

$$+ \frac{\partial U}{\partial R}\left(U(R_r^2 + R_\theta^2 + \frac{4}{3}R_z^2) + \frac{1}{3}R_\theta R_z V + \frac{1}{3}R_r R_z W\right) + \frac{\partial V}{\partial n}\left(V(R_r n_r + \frac{4}{3}R_\theta n_\theta + R_z n_z)\right.$$

$$\left. + U(R_\theta n_z - \frac{2}{3}R_z n_\theta) + W(R_\theta n_r - \frac{2}{3}R_r n_\theta)\right) + \frac{\partial V}{\partial R}\left(V(R_r^2 + \frac{4}{3}R_\theta^2 + R_z^2)\right.$$

$$\left. + \frac{R_z R_\theta}{3}U + \frac{R_\theta R_r}{3}W\right) + \frac{\partial W}{\partial n}\left(W(\frac{4}{3}n_r R_r + n_\theta R_\theta + n_z R_z) + U(n_z R_r - \frac{2}{3}n_r R_z)\right.$$

$$\left. + V(n_\theta R_r - \frac{2}{3}R_\theta n_r)\right) + \frac{\partial W}{\partial R}\left(W(\frac{4}{3}R_r^2 + R_\theta^2 + R_z^2) + \frac{R_r R_z}{3}U + \frac{R_\theta R_r V}{3}\right)$$

$$\left. + \frac{1}{R}(-V^2 R_r + \frac{VWR_\theta}{3} - \frac{2}{3}UWR_z)\right] + \frac{\gamma}{P_r J}\left((R_r n_r + n_\theta R_\theta + n_z R_z)\frac{\partial e_i}{\partial n} + (R_r^2 + R_\theta^2\right.$$

$$\left. + R_z^2)\frac{\partial e_i}{\partial R}\right)$$

$$Q_1 = 0$$

$$Q_2 = \frac{\mu}{J}\left[(n_r^2 + n_\theta^2 + \frac{4}{3}n_z^2)\frac{\partial U}{\partial n} + \frac{n_\theta n_z}{3}\frac{\partial V}{\partial n} + \frac{n_z n_r}{3}\frac{\partial W}{\partial n} + (n_r R_r + n_\theta R_\theta + \frac{4}{3}n_z R_z)\frac{\partial U}{\partial R}\right.$$

$$\left. + (n_\theta R_r - \frac{2}{3}n_z R_\theta)\frac{\partial V}{\partial R} + (n_z R_r - \frac{2}{3}n_z R_r)\frac{\partial W}{\partial R} - \frac{2}{3}n_z\frac{W}{R}\right]$$

$$Q_3 = \frac{\mu}{J}\left[\frac{n_z n_\theta}{3}\frac{\partial U}{\partial n} + (n_r^2 + \frac{4}{3}n_\theta^2 + n_z^2)\frac{\partial V}{\partial n} + \frac{n_r n_\theta}{3}\frac{\partial W}{\partial n} + (R_\theta n_z - \frac{2}{3}R_z n_\theta)\frac{\partial U}{\partial R}\right.$$

$$\left. + (n_r R_r + \frac{4}{3}n_\theta R_\theta + n_z R_z)\frac{\partial V}{\partial R} + (n_r R_\theta - \frac{2}{3}R_r n_\theta)\frac{\partial W}{\partial R} - n_r\frac{V}{R} + \frac{4}{3}n_\theta\frac{W}{R}\right]$$

$$Q_4 = \frac{\mu}{J}\left[\frac{n_z n_r}{3}\frac{\partial U}{\partial n} + \frac{n_\theta n_r}{3}\frac{\partial V}{\partial n} + (\frac{4}{3} n_r^2 + n_\theta^2 + n_z^2)\frac{\partial W}{\partial n} + (n_r R_r - \frac{2}{3} n_r R_r)\frac{\partial U}{\partial R}\right.$$

$$\left. + (n_\theta R_r - \frac{2}{3} n_r R_\theta)\frac{\partial V}{\partial R} + (\frac{4}{3} n_r R_r + n_\theta R_\theta + n_z R_z)\frac{\partial W}{\partial R} - \frac{2}{3} n_r \frac{W}{R} - n_\theta \frac{V}{R}\right]$$

$$Q_5 = \frac{\mu}{J}\left[\frac{\partial U}{\partial n}\left(U(n_r^2 + n_\theta^2 + \frac{4}{3} n_z^2) + \frac{n_\theta n_z V}{3} + \frac{n_r n_z W}{3}\right) + \frac{\partial U}{\partial R}\left(U(n_r R_r + n_\theta R_\theta + \frac{4}{3} n_z R_z)\right.\right.$$

$$\left. + V(n_z R_\theta - \frac{2}{3} n_\theta R_z) + W(n_z R_z + \frac{2}{3} n_r R_z)\right) + \frac{\partial V}{\partial n}\left(V(n_r^2 + \frac{4}{3} n_\theta^2 + n_z^2)\right.$$

$$\left. + \frac{n_z n_\theta}{3} U + \frac{n_\theta n_r}{3} W\right) + \frac{\partial V}{\partial R}\left(V(n_r R_r + \frac{4}{3} n_\theta R_\theta + n_z R_z) + U(n_\theta R_z - \frac{2}{3} n_z R_\theta)\right.$$

$$\left. + W(n_\theta R_r - \frac{2}{3} n_r R_\theta)\right) + \frac{\partial W}{\partial n}\left(W(\frac{4}{3} n_r^2 + n_\theta^2 + n_z^2) + \frac{n_z n_r U}{3} + \frac{n_\theta n_r V}{3}\right)$$

$$+ \frac{\partial W}{\partial R}\left(W(n_z R_z + n_\theta R_\theta + \frac{4}{3} n_r R_r) + U(R_z n_r - \frac{2}{3} R_r n_z) + V(R_\theta n_r - \frac{2}{3} n_\theta R_r)\right)$$

$$\left. + \frac{1}{R}(-V^2 n_r + \frac{V W n_\theta}{3} - \frac{2}{3} U W n_z)\right] + \frac{\gamma}{P_r J}\left[(n_r^2 + n_\theta^2 + n_z^2)\frac{\partial e_i}{\partial n}\right.$$

$$\left. + (n_r R_r + n_\theta R_\theta + n_z R_z)\frac{\partial e_i}{\partial R}\right]$$

$$S_1 = 0$$

$$S_2 = \frac{\mu}{R}(n_r \frac{\partial U}{\partial n} + R_r \frac{\partial U}{\partial R} + n_z \frac{\partial W}{\partial n} + R_r \frac{\partial W}{\partial R})$$

$$S_3 = \frac{2\mu}{R}(n_\theta \frac{\partial W}{\partial n} + R_\theta \frac{\partial W}{\partial R} + n_r \frac{\partial V}{\partial n} + R_r \frac{\partial V}{\partial R} - \frac{V}{R})$$

$$S_4 = \frac{2\mu}{R}(n_r \frac{\partial W}{\partial n} + R_r \frac{\partial W}{\partial R} - n_\theta \frac{\partial V}{\partial n} - R_\theta \frac{\partial V}{\partial R} - \frac{W}{R})$$

$$S_5 = \frac{\mu}{R}\left[\frac{\partial U}{\partial n}(U n_r - \frac{2}{3} W n_z) + \frac{\partial U}{\partial R}(U R_r - \frac{2}{3} W R_z) + \frac{\partial V}{\partial n}(V n_r - \frac{2}{3} W n_\theta) + \frac{\partial V}{\partial R}(V R_r - \frac{2}{3} W R_\theta)\right.$$

$$\left. + \frac{\partial W}{\partial n}(\frac{4}{3} W n_r + n_\theta V + n_z U) + \frac{\partial W}{\partial R}(\frac{4}{3} W R_r + R_\theta V + R_z U) - \frac{1}{R}(V^2 + \frac{2}{3} W^2)\right]$$

$$+ \frac{\gamma}{P_r R}(\frac{\partial e_i}{\partial n} + R_r \frac{\partial e_i}{\partial R})$$

The Jacobian Matrix of the Vector E

$e_{11} = 0$

$e_{12} = \xi_z$

$e_{13} = \xi_n$

$e_{14} = \xi_r$

$e_{15} = 0$

$e_{21} = 0$

$e_{22} = 2U\xi_z + V\xi_\theta + W\xi_r$

$e_{23} = \xi_\theta U$

$e_{24} = \xi_r U$

$e_{25} = -U^2\xi_z + \xi_\theta UV - \xi_r WU$

$e_{31} = 0$

$e_{32} = V\xi_z$

$e_{33} = U\xi_z + 2V\xi_\theta + W\xi_r$

$e_{34} = \xi_r V$

$e_{35} = -UV\xi_z - V^2\xi_\theta - UW\xi_r$

$e_{41} = 0$

$e_{42} = W\xi_z$

$e_{43} = W\xi_\theta$

$e_{44} = U\xi_z + V\xi_\theta + 2W\xi_r$

$e_{45} = -UW\xi_z - VW\xi_\theta - W^2\xi_r$

$e_{51} = \gamma(\xi_z U + \xi_\theta V + \xi_r W)$

$$e_{52} = \gamma\xi_z e_i + \frac{3}{2}\xi_z U^2 + \xi_\theta UV + \xi_r UW + \frac{\xi_z}{2}(V^2 + W^2)$$

$$e_{53} = \gamma\xi_\theta e_i + \xi_2 VU + \frac{3}{2}\xi_\theta V^2 + \xi_r VW + \frac{\xi_\theta}{2}(U^2 + W^2)$$

$$e_{54} = \gamma\xi_r e_i + \xi_z WU + \xi_\theta WV + \frac{3}{2}\xi_r W^2 + \frac{\xi_r}{2}(U^2 + V^2)$$

$$e_{55} = -\gamma e_i(\xi_z U + \xi_\theta V + \xi_r W) - \xi_z(U^2 + UV + UW) - \xi_\theta(VU + V^2 + VW) - \xi_r(WU + WV + W^2)$$

The Jacobian Matrix of Vector F

$$f_{11} = 0$$

$$f_{12} = n_z$$

$$f_{13} = n_\theta$$

$$f_{14} = n_r$$

$$f_{15} = 0$$

$$f_{21} = n_z(\gamma-1)$$

$$f_{22} = 2Un_z + Vn_\theta + Wn_r$$

$$f_{23} = n_\theta U$$

$$f_{24} = n_r U$$

$$f_{25} = -U^2 n_z - UVn_\theta - UWn_r$$

$$f_{31} = n\ (\gamma-1)$$

$$f_{32} = Vn_z$$

$$f_{33} = Un_z + 2Vn_\theta + Wn_r$$

$$f_{34} = n_r V$$

$$f_{35} = -UVn_z - V^2 n_\theta - VWn_r$$

$$f_{41} = n_r(\gamma-1)$$

$$f_{42} = Vn_z$$

$$f_{43} = Un_z + 2Vn_\theta + Wn_r$$

$$f_{44} = n_r V$$

$$f_{45} = -UWn_z - VWn_\theta - W^2 n_r$$

$$f_{51} = \gamma(n_z U + n_\theta V + n_r W)$$

$$f_{52} = \gamma n_z e_i + \frac{3}{2} U^2 + n_\theta UV + n_r UW + \frac{n_z}{2}(V^2 + W^2)$$

$$f_{53} = \gamma n_\theta e_i + n_z VU + \frac{3}{2} n_\theta V^2 + n_r VW + \frac{n_\theta}{2}(U^2 + W^2)$$

$$f_{54} = \gamma n_r e_i + n_z WU + n_\theta WV + \frac{3}{2} n_r W^2 + \frac{n_r}{2}(U^2 + V^2)$$

$$f_{55} = -\gamma e_i(n_z U + n_\theta V + n_r W) - n_z(U^2 + UV + UW) - n_\theta(VU + V^2 + VW) - n_r(WU + WV + W^2)$$

The Jacobian Matrix of the Vector G

$g_{11} = 0$

$g_{12} = R_z$

$g_{13} = R_\theta$

$g_{14} = R_r$

$g_{15} = 0$

$g_{21} = R_z(\gamma-1)$

$g_{22} = 2UR_z + VR_\theta + WR_r$

$g^{23} = R_\theta U$

$g_{24} = R_r U$

$g_{25} = -U^2R_z - UVR_\theta - UWR_r$

$g_{31} = R_\theta(\gamma-1)$

$g_{32} = VR_z$

$g_{33} = VR_\theta$

$g_{34} = UR_z + VR_\theta + 2WR_r$

$g_{35} = UVR_z - V^2R_\theta - VWR_r$

$g_{41} = R_r(\gamma-1)$

$g_{42} = WR_z$

$g_{43}\ WR_\theta$

$g_{44} = UR_z + VR_\theta + 2WR_r$

$g_{45} = -UWR_z - VWR_\theta - W^2R_r$

$g_{51} = \gamma(R_zU + R_\theta V - R_rW)$

$g_{52} = \gamma R_z e_i + \frac{3}{2}R_z\ U^2 + R_\theta UV + R_rUW + \frac{R_z}{2}(V^2 + W^2)$

$g_{53} = \gamma R_\theta e_i + R_zVU + \frac{3}{2}\ R\ V^2 + R_rVW + \frac{R_\theta}{2}(U^2 + W^2)$

$g_{54} = \gamma R_r e_i + R_zWU + R_\theta WV + \frac{3}{2}\ R_rW^2 + \frac{R_r}{2}(U^2 + V^2)$

$$g_{55} = -\gamma e_i(R_zU + R_\theta V + R_rW) - R_z(U^2 + UV + UW) - R_\theta(VU + V^2 + VW)$$
$$-R_r(WU + WV + W^2)$$

The Jacobian Matrix of the Vector C

$$c_{11} = 0$$

$$c_{12} = 0$$

$$c_{13} = 0$$

$$c_{14} = \frac{J}{\rho R}$$

$$c_{15} = -\frac{JW}{R}$$

$$c_{21} = 0$$

$$c_{22} = W$$

$$c_{23} = 0$$

$$c_{24} = U$$

$$c_{25} = -UW$$

$$c_{31} = 0$$

$$c_{32} = 0$$

$$c_{33} = \frac{2WJ}{R}$$

$$c_{34} = \frac{2J(V + \Omega R)}{R}$$

$$c_{35} = -\frac{VWJ}{R}$$

$$c_{41} = c_{42} = 0$$

$$c_{43} = (-2V - 2\Omega R)\frac{J}{R}$$

$$c_{44} = 2WJ/R$$

$$c_{45} = (-W^2 + V^2 - \Omega^2 R^2)\frac{J}{R}$$

$$c_{51} = \frac{J}{R}\gamma W$$

$$c_{52} = \frac{J}{R} UW$$

$$c_{53} = \frac{J}{R} VW$$

$$c_{54} = \frac{J}{R}(2W^2 + U^2 + V^2 + \gamma e_i - \Omega^2 R^2)$$

$$c_{55} = \frac{J}{R}(-\gamma W e_i - UW - VW - W^2)$$

The Jacobian Matrix of the Vector P

$$P_{11} = P_{12} = P_{13} = P_{14} = P_{15} = 0$$

$$P_{21} = 0$$

$$P_{22} = \mu(R_r^2 + R_\theta^2 + \frac{4}{3} R_z^2) \frac{\partial}{\partial R} \left[\frac{1}{\rho} \right]$$

$$P_{23} = \mu \frac{R_\theta R_z}{3} \frac{\partial}{\partial R} \left[\frac{1}{\rho} \right]$$

$$P_{24} = \mu(\frac{R_r R_z}{3} \frac{\partial}{\partial R} \left[\frac{1}{\rho} \right] - \frac{2}{3} \frac{R_z}{\rho R})$$

$$P_{25} = \mu(-(R_r^2 + R_\theta^2 + \frac{4}{3} R_z^2) \frac{\partial}{\partial R} \left[\frac{U}{\rho} \right] \frac{R_\theta R_z}{3} \frac{\partial}{\partial R} \left[\frac{V}{\rho} \right] - \frac{R_r R_z}{3} \frac{\partial}{\partial R} \left[\frac{W}{\rho} \right]$$
$$+ \frac{2R_z}{3} \frac{W}{\rho R})$$

$$P_{31} = 0$$

$$P_{32} = \mu \frac{R_\theta R_z}{3} \frac{\partial}{\partial R} \left[\frac{1}{\rho} \right]$$

$$P_{33} = \mu \left[(R_r^2 + \frac{4}{3} R_\theta^2 + R_z^2) \frac{\partial}{\partial R} \left[\frac{1}{\rho} \right] - \frac{R_r}{\rho R} \right]$$

$$P_{34} = \mu \left[\frac{R_r R_\theta}{3} \frac{\partial}{\partial R} \left[\frac{1}{\rho} \right] + \frac{4}{3} \frac{R_\theta}{\rho R} \right]$$

$$P_{35} = \mu \left[-\frac{R_\theta R_z}{3} \frac{\partial}{\partial R} \left[\frac{U}{\rho} \right] - (R_r^2 + \frac{4}{3} R_\theta^2 + R_z^2) \frac{\partial}{\partial R} \left[\frac{V}{\rho} \right] - \frac{R_r R_\theta}{3} \frac{\partial}{\partial R} \left[\frac{W}{\rho} \right] \right.$$
$$\left. + R_r \frac{V}{\rho R} - \frac{4}{3} \frac{R_\theta W}{\rho R} \right]$$

$$P_{41} = 0$$

$$P_{42} = \mu(-\frac{R_\theta R_z}{3} \frac{\partial}{\partial R} \left[\frac{1}{\rho} \right])$$

$$P_{43} = \mu(-\frac{R_r R_\theta}{3} \frac{\partial}{\partial R} \left[\frac{1}{\rho} \right] - \frac{R_\theta}{\rho R})$$

$$P_{44} = \mu((\frac{4}{3} R_r^2 + R_\theta^2 + R_z^2) \frac{\partial}{\partial R} \left[\frac{1}{\rho} \right] - \frac{2}{3} R_r \frac{1}{\rho R})$$

$$P_{45} = \mu\Big[-\frac{R_rR_z}{3}\frac{\partial}{\partial R}\Big[\frac{U}{\rho}\cdot\Big] - \frac{R_rR_\theta}{3}\frac{\partial}{\partial R}\Big[\frac{V}{\rho}\cdot\Big] - (\frac{4}{3}R_r^2 + R_\theta^2 + R_z^2)\frac{\partial}{\partial R}(\frac{W}{\rho}\cdot)$$

$$+ \frac{2}{3}R_r\frac{W}{\rho R} + R_\theta\frac{V}{\rho R}\Big]$$

$$P_{51} = \frac{\gamma}{P_r}\Big[(R_r^2 + R_\theta^2 + R_z^2)\frac{\partial}{\partial R}\Big[\frac{1}{\rho}\cdot\Big]\Big]$$

$$P_{52} = \mu\Big[(R_r^2 + R_\theta^2 + \frac{4}{3}R_z^2)(U\frac{\partial}{\partial R}\Big[\frac{1}{\rho}\cdot\Big] + \frac{1}{\rho}\frac{\partial U}{\partial R}) + \frac{R_\theta R_z}{3}V\frac{\partial}{\partial R}\Big[\frac{1}{\rho}\cdot\Big]$$

$$+ \frac{R_rR_z}{3}W\frac{\partial}{\partial R}\Big[\frac{1}{\rho}\cdot\Big] + \frac{R_\theta R_z}{3}\frac{1}{\rho}\frac{\partial V}{\partial R} + \frac{R_rR_z}{3}\frac{1}{\rho}\frac{\partial W}{\partial R} - \frac{2}{3}\frac{WR_z}{\rho R}\Big]$$

$$P_{53} = \mu\Big[(R_r^2 + \frac{4}{3}R_\theta^2 + R_z^2)(V\frac{\partial}{\partial R}\Big[\frac{1}{\rho}\cdot\Big] + \frac{1}{\rho}\frac{\partial V}{\partial R}) + \frac{R_zR_\theta}{3}U\frac{\partial}{\partial R}\Big[\cdot\frac{1}{\rho}\cdot\Big]$$

$$+ \frac{R_\theta R_r}{3}W\frac{\partial}{\partial R}\Big[\frac{1}{\rho}\cdot\Big] + \frac{R_zR_\theta}{3}\frac{1}{\rho}\frac{\partial U}{\partial R} + \frac{R_\theta R_r}{3}\frac{1}{\rho}\frac{\partial W}{\partial R} + \frac{WR_\theta}{3\rho R} - \frac{2VR_r}{\rho R}\Big]$$

$$P_{54} = \mu\Big[(\frac{4}{3}R_r^2 + R_\theta^2 + R_z^2)(W\frac{\partial}{\partial R}\Big[\frac{1}{\rho}\cdot\Big] + \frac{1}{\rho}\frac{\partial W}{\partial R}) + \frac{R_rR_z}{3}U\frac{\partial}{\partial R}\Big[\frac{1}{\rho}\cdot\Big]$$

$$+ \frac{R_\theta R_rV}{3}\frac{\partial}{\partial R}\Big[\frac{1}{\rho}\cdot\Big] + \frac{R_rR_z}{3}\frac{1}{\rho}\frac{\partial U}{\partial R} + \frac{R_\theta R_r}{3}\frac{1}{\rho}\frac{\partial V}{\partial R} + \frac{VR_\theta}{3\rho R} - \frac{2}{3}\frac{UR_z}{\rho R})$$

$$P_{55} = \frac{\gamma}{P_r}(-(R_r^2 + R_\theta^2 + R_z^2)\frac{\partial}{\partial R}\Big[\frac{e_i}{p}\Big]) - \mu\Big[(R_r^2 + R_\theta^2 + \frac{4}{3}R_z^2)(U\frac{\partial}{\partial R}(\frac{U}{\rho}\cdot)$$

$$+ \frac{U}{\rho}\frac{\partial U}{\partial R}) + \frac{R_\theta R_z}{3}(V\frac{\partial}{\partial R}(\frac{U}{\rho}\cdot) + \frac{V}{\rho}\frac{\partial U}{\partial R}) + \frac{R_rR_z}{3}(W\frac{\partial}{\partial R}(\frac{U}{\rho}\cdot) + \frac{W}{\rho}\frac{\partial U}{\partial R})$$

$$+ (R_r^2 + \frac{4}{3}R_\theta^2 + R_z^2)(V\frac{\partial}{\partial R}\Big[\frac{V}{\rho}\cdot\Big] + \frac{V}{\rho}\frac{\partial V}{\partial R}) + \frac{R_zR_\theta}{3}(U\frac{\partial}{\partial R}\Big[\frac{V}{\rho}\cdot\Big]$$

$$+ \frac{U}{\rho}\frac{\partial V}{\partial R}) + \frac{R_\theta R_r}{3}(W\frac{\partial}{\partial R}\Big[\frac{V}{\rho}\cdot\Big] + \frac{W}{\rho}\frac{\partial V}{\partial R}) + (\frac{4}{3}R_r^2 + R_\theta^2 + R_z^2)$$

$$(W\frac{\partial}{\partial R}\Big[\frac{W}{\rho}\Big] + \frac{W}{\rho}\frac{\partial W}{\partial R}) + \frac{R_rR_z}{3}(U\frac{\partial}{\partial R}\Big[\frac{W}{\rho}\cdot\Big] + \frac{U}{\rho}\frac{\partial W}{\partial R}) + \frac{R_\theta R_r}{3}$$

$$(V\frac{\partial}{\partial R}\Big[\frac{W}{\rho}\Big] + \frac{V}{\rho}\frac{\partial W}{\partial R}) + \frac{1}{\rho}(\frac{-2V^2}{\rho}R_r + \frac{VW}{3\rho}R_\theta - \frac{2UWR_z}{3\rho})\Big]$$

The Jacobian Matrix of the Vector Q

$$q_{11} = q_{12} = q_{13} = q_{14} = q_{15} = 0$$

$$q_{21} = 0$$

ORIGINAL PAGE IS OF POOR QUALITY

$$q_{22} = \mu(n_r^2 + n_\theta^2 + \frac{4}{3} n_z^2) \frac{\partial}{\partial n} \left[\frac{1}{\rho}.\right]$$

$$q_{23} = \mu \frac{n_\theta n_z}{3} \frac{\partial}{\partial n} \left[\frac{1}{\rho}.\right]$$

$$q_{24} = \mu \frac{n_z n_r}{3} \frac{\partial}{\partial n} \left[\frac{1}{\rho}.\right] - \frac{2}{3} \frac{n_z}{\rho R}$$

$$q_{25} = -\mu\left((n_r^2 + n_\theta^2 + \frac{4}{3} n_z^2) \frac{\partial}{\partial n} \left[\frac{U}{\rho}.\right] + \frac{n_\theta n_z}{3} \frac{\partial}{\partial n} \left[\frac{V}{\rho}.\right] + \frac{n_z n_r}{3} \frac{\partial}{\partial n} \left[\frac{W}{\rho}.\right] + \frac{2n_z}{3} \frac{W}{\rho R}\right)$$

$$q_{31} = 0$$

$$q_{32} = \mu \frac{n_z n_\theta}{3} \frac{\partial}{\partial n} \left[\frac{1}{\rho}.\right]$$

$$q_{33} = \mu(n_r^2 + \frac{4}{3} n_\theta^2 + n_z^2) \frac{\partial}{\partial n} \left[\frac{1}{\rho}\right] - \frac{n_r}{\rho R}$$

$$q_{34} = \mu(\frac{n_r n_\theta}{3} \frac{\partial}{\partial n} \left[\frac{1}{\rho}.\right] + \frac{4}{3} \frac{n_\theta}{\rho R})$$

$$q_{35} = \mu(-\frac{n_z n_\theta}{3} \frac{\partial}{\partial n} \left[\frac{U}{\rho}.\right] - (n_r^2 + \frac{4}{3} n_\theta^2 + n_z^2) \frac{\partial}{\partial n} \left[\frac{V}{\rho}.\right] - \frac{n_r n_\theta}{3} \frac{\partial}{\partial n} \left[\frac{W}{\rho}.\right]$$
$$+ n_r \frac{V}{\rho R} - \frac{4}{3} \frac{n_\theta W}{\rho R})$$

$$q_{41} = 0$$

$$q_{42} = \mu \frac{n_z n_r}{3} \frac{\partial}{\partial n} \left[\frac{1}{\rho}.\right]$$

$$q_{43} = \frac{n_\theta n_r}{3} \frac{\partial}{\partial n} \left[\frac{1}{\rho}.\right]$$

$$q_{44} = \mu\left((\frac{4}{3} n_r^2 + n_\theta^2 + n_z^2) \frac{\partial}{\partial n} \left[\frac{1}{\rho}.\right] - \frac{2}{3} n_r \frac{1}{\rho R}\right)$$

$$q_{45} = \mu(- \frac{n_z n_r}{3} \frac{\partial}{\partial n} \left[\frac{U}{\rho}.\right] - \frac{n_\theta n_r}{3} \frac{\partial}{\partial n} \left[\frac{V}{\rho}.\right] - (\frac{4}{3} n_r^2 + n_\theta^2 + n_z^2) \frac{\partial}{\partial n} \left[\frac{W}{\rho}.\right]$$
$$+ \frac{2}{3} n_r \frac{W}{\rho R} + n_\theta \frac{V}{\rho R})$$

$$q_{51} = \frac{\gamma}{P_r}(n_r^2 + n_\theta^2 + n_z^2)\frac{\partial}{\partial n}\left[\frac{1}{\rho}\cdot\right]$$

$$q_{52} = \mu\Big((n_r^2 + n_\theta^2 + \frac{4}{3}n_z^2)(U\frac{\partial}{\partial n}\left[\frac{1}{\rho}\cdot\right] + \frac{1}{\rho}\frac{\partial U}{\partial n}) + \frac{n_\theta n_z}{3} V \frac{\partial}{\partial n}\left[\frac{1}{\rho}\cdot\right]$$

$$+ \frac{n_r n_z}{3} W \frac{\partial}{\partial n}\left[\frac{1}{\rho}\cdot\right] + \frac{n_z n_r}{3}\frac{1}{\rho}\frac{\partial W}{\partial n} - \frac{2}{3} n_z \frac{W}{\rho R}\Big)$$

$$q_{53} = \mu\Big((n_r^2 + \frac{4}{3}n_\theta^2 + n_z^2)(V\frac{\partial}{\partial n}\left[\frac{1}{\rho}\cdot\right] + \frac{1}{\rho}\frac{\partial V}{\partial n}) + \frac{n_z n_\theta}{3} U \frac{\partial}{\partial n}\left[\frac{1}{\rho}\cdot\right]$$

$$+ \frac{n_\theta n_r}{3} W \frac{\partial}{\partial n}\left[\frac{1}{\rho}\cdot\right] + \frac{n_\theta n_z}{3}\frac{1}{\rho}\frac{\partial U}{\partial n} + \frac{n_\theta n_r}{3}\frac{1}{\rho}\frac{\mu W}{\partial n} - \frac{2V}{\rho}\frac{n_r}{R} + \frac{W}{3\rho}\frac{n_\theta}{R}\Big)$$

$$q_{54} = \mu\Big((\frac{4}{3}n_r^2 + n_\theta^2 + n_z^2)(W\frac{\partial}{\partial n}\left[\frac{1}{\rho}\cdot\right] + \frac{1}{\rho}\frac{\partial W}{\partial n}) + \frac{n_z n_r}{3} U \frac{\partial}{\partial n}\left[\frac{1}{\rho}\cdot\right]$$

$$+ \frac{n_\theta n_r}{3} V\frac{\partial}{\partial n}\left|\frac{1}{\rho}\cdot\right| + \frac{n_r n_z}{3}\frac{1}{\rho}\frac{\partial U}{\partial n} + \frac{n_\theta n_r}{3\rho}\frac{\partial V}{\partial n} + \frac{n_\theta}{3R}\frac{V}{\rho} - \frac{n_z}{R}\frac{U}{\rho}\Big)$$

$$q_{55} = -\frac{\gamma}{P_r}(n_r^2 + n_\theta^2 + n_z^2)\frac{\partial}{\partial n}\left[\frac{e_i}{\rho}\cdot\right] - \mu\Big((n_r^2 + n_\theta^2 + \frac{4}{3}n_z^2)(U\frac{\partial}{\partial n}\left[\frac{U}{\rho}\cdot\right]$$

$$+ \frac{U}{\rho}\frac{\partial U}{\partial n}) + \frac{n_\theta n_z}{3}(V\frac{\partial}{\partial n}\left[\frac{U}{\rho}\cdot\right] + \frac{V}{\rho}\frac{\partial U}{\partial n}) + \frac{n_r n_z}{3}(W\frac{\partial}{\partial n}\left[\frac{U}{\rho}\cdot\right]$$

$$+ \frac{W}{\rho}\frac{\partial U}{\partial n}) + (n_r^2 + \frac{4}{3}n_\theta^2 + n_z^2)(V\frac{\partial}{\partial n}\left[\frac{1}{\rho}\cdot\right] + \frac{V}{\rho}\frac{\partial V}{\partial n})$$

$$+ \frac{n_z n_\theta}{3}(U\frac{\partial}{\partial n}\left[\frac{V}{\rho}\cdot\right] + \frac{U}{\rho}\frac{\partial V}{\partial n}) + \frac{n_\theta n_r}{3}(W\frac{\partial}{\partial n}\left[\frac{V}{\rho}\cdot\right] + \frac{W}{\rho}\frac{\partial V}{\partial n})$$

$$+ (\frac{4}{3}n_r^2 + n_\theta^2 + n_z^2)(W\frac{\partial}{\partial n}\left[\frac{W}{\rho}\cdot\right] + \frac{W}{\rho}\frac{\partial W}{\partial n}) + \frac{n_z n_r}{3}(U\frac{\partial}{\partial n}\left[\frac{W}{\rho}\cdot\right]$$

$$+ \frac{U}{\rho}\frac{\partial W}{\partial n}) + \frac{n_\theta n_r}{3}(V\frac{\partial}{\partial n}\left[\frac{W}{\rho}\cdot\right] + \frac{V}{\rho}\frac{\partial W}{\partial n}) + \frac{1}{R}(-\frac{2V^2}{\rho}n_r + \frac{VW}{3\rho}n_\theta - \frac{2UWn_z}{3\rho})\Big)$$

The Jacobian Matrix of the Vector S

$$s_{11} = s_{12} = s_{13} = s_{14} = s_{15} = 0$$

$$s_{21} = 0$$

$$s_{22} = \frac{\mu J}{R} (n_r \frac{\partial}{\partial n} \left[\frac{1}{\rho}. \right] + R_r \frac{\partial}{\partial R} \left[\frac{1}{\rho}. \right])$$

$$s_{23} = 0$$

$$s_{24} = \frac{\mu J}{R} (n_z \frac{\partial}{\partial n} \left[\frac{1}{\rho}. \right] + R_r \frac{\partial}{\partial R} \left[\frac{1}{\rho}. \right])$$

$$s_{25} = \frac{\mu J}{R} (-n_r \frac{\partial}{\partial n} \left[\frac{U}{\rho}. \right] - R_r \frac{\partial}{\partial R} \left[\frac{U}{\rho}. \right] - n_z \frac{\partial}{\partial n} \left[\frac{W}{\rho}. \right] - R_r \frac{\partial}{\partial R} \left[\frac{W}{\rho}. \right])$$

$$s_{31} = 0$$

$$s_{32} = 0$$

$$s_{33} = \frac{2\mu J}{R} (n_r \frac{\partial}{\partial n} \left[\frac{1}{\rho}. \right] + R_r \frac{\partial}{\partial R} \left[\frac{1}{\rho}. \right] - \frac{1}{\rho R})$$

$$s_{34} = \frac{2\mu J}{R} (n_\theta \frac{\partial}{\partial n} \left[\frac{1}{\rho}. \right] + R_\theta \frac{\partial}{\partial R} \left[\frac{1}{\rho}. \right])$$

$$s_{35} = \frac{2\mu J}{R} (-n_\theta \frac{\partial}{\partial n} \left[\frac{W}{\rho}. \right] - R_\theta \frac{\partial}{\partial R} \left[\frac{W}{\rho}. \right] - n_r \frac{\partial}{\partial n} \left[\frac{V}{\rho}. \right] - R_r \frac{\partial}{\partial R} \left[\frac{V}{\rho}. \right] + \frac{V}{\rho R}$$

$$s_{41} = s_{42} = 0$$

$$s_{43} = \frac{-2\mu J}{R} (n_\theta \frac{\partial}{\partial n} \left[\frac{1}{\rho}. \right] + R_\theta \frac{\partial}{\partial R} \left[\frac{1}{\rho}. \right])$$

$$s_{44} = \frac{2\mu J}{R} (n_r \frac{\partial}{\partial n} \left[\frac{1}{\rho}. \right] + R_r \frac{\partial}{\partial R} \left[\frac{1}{\rho}. \right])$$

$$s_{45} = \frac{2\mu J}{R} (-n_r \frac{\partial}{\partial n} \left[\frac{W}{\rho}. \right] - R_r \frac{\partial}{\partial R} \left[\frac{W}{\rho}. \right] + n_\theta \frac{\partial}{\partial n} \left[\frac{V}{\rho}. \right] + R_\theta \frac{\partial}{\partial R} \left[\frac{V}{\rho}. \right] + \frac{W}{\rho R})$$

$$s_{51} = \frac{\gamma}{RP_r} (n_r \frac{\partial}{\partial n} \left[\frac{1}{\rho}. \right] + R_r \frac{\partial}{\partial R} \left[\frac{1}{\rho}. \right])$$

$$s_{52} = \frac{\mu J}{R} \Big(n_r (U \frac{\partial}{\partial n} \left[\frac{1}{\rho}. \right] + \frac{1}{\rho} \frac{\partial U}{\partial n}) - \frac{2}{3} n_z W \frac{\partial}{\partial n} \left[\frac{1}{\rho}. \right] + R_r (U \frac{\partial}{\partial R} \left[\frac{1}{\rho}. \right] + \frac{1}{\rho} \frac{\partial U}{\partial R})$$

$$- \frac{2}{3} R_z W \frac{\partial}{\partial R} \left[\frac{1}{\rho}. \right] + n_z \frac{1}{\rho} \frac{\partial W}{\partial n} + R_z \frac{1}{\rho} \frac{\partial W}{\partial R}\Big)$$

$$s_{53} = \frac{\mu J}{R} \Big(n_r (V \frac{\partial}{\partial n} \left[\frac{1}{\rho}. \right] + \frac{1}{\rho} \frac{\partial V}{\partial n}) - \frac{2}{3} n_\theta W \frac{\partial}{\partial n} \left[\frac{1}{\rho}. \right] + R_r (V \frac{\partial}{\partial R} \left[\frac{1}{\rho}. \right] + \frac{1}{\rho} \frac{\partial V}{\partial R})$$

$$- \frac{2}{3} R_\theta W \frac{\partial}{\partial R} \left[\frac{1}{\rho}. \right] + n_\theta \frac{1}{\rho} \frac{\partial W}{\partial n} + R_\theta \frac{1}{\rho} \frac{\partial W}{\partial R} - \frac{2V}{\rho R} \Big)$$

$$s_{54} = \frac{\mu J}{R} \Big(\frac{4}{3} n_r (W \frac{\partial}{\partial n} \left[\frac{1}{\rho}. \right] + \frac{1}{\rho} \frac{\partial W}{\partial n}) + n_\theta V \frac{\partial}{\partial n} \left[\frac{1}{\rho}. \right] + n_z U \frac{\partial}{\partial n} \left[\frac{1}{\rho}. \right]$$

$$+ \frac{4}{3} R_r (W \frac{\partial}{\partial R} \left[\frac{1}{\rho}. \right] + \frac{1}{\rho} \frac{\partial W}{\partial R}) + R_\theta V \frac{\partial}{\partial R} \left[\frac{1}{\rho}. \right] + R_z U \frac{\partial}{\partial R} \left[\frac{1}{\rho}. \right]$$

$$- \frac{2}{3} \frac{n_\theta}{\rho} \frac{\partial V}{\partial n} - \frac{2R_\theta}{3\rho} \frac{\partial V}{\partial R} - \frac{2}{3} \frac{n_z}{\rho} \frac{\partial U}{\partial n} - \frac{2}{3} \frac{R_z}{\rho} \frac{\partial U}{\partial R} - \frac{4}{3} \frac{W}{\rho R} \Big)$$

$$s_{55} = \frac{\gamma}{RP_r} (n_r \frac{\partial}{\partial n} \left[\frac{e_i}{\rho}. \right] + R_r \frac{\partial}{\partial R} \left[\frac{e_i}{\rho}. \right]) - \frac{\mu J}{R} \Big(n_r (U \frac{\partial}{\partial n} \left[\frac{U}{\rho}. \right] + \frac{U}{\rho} \frac{\partial U}{\partial n})$$

$$- \frac{2}{3} n_z (W \frac{\partial}{\partial n} \left[\frac{U}{\rho}. \right] + \frac{W}{\rho} \frac{\partial U}{\partial n}) + R_r (U \frac{\partial}{\partial R} \left[\frac{U}{\rho}. \right] + \frac{U}{\rho} \frac{\partial U}{\partial n}) - \frac{2}{3} R_z$$

$$(W \frac{\partial}{\partial R} \left[\frac{U}{\rho}. \right] + \frac{W}{\rho} \frac{\partial U}{\partial R}) + n_r (V \frac{\partial}{\partial n} \left[\frac{V}{\rho}. \right] + \frac{V}{\rho} \frac{\partial V}{\partial n}) - \frac{2}{3} n_\theta (W \frac{\partial}{\partial n} \left[\frac{V}{\rho}. \right]$$

$$+ \frac{W}{\rho} \frac{\partial V}{\partial n}) + R_r (V \frac{\partial}{\partial R} \left[\frac{V}{\rho}. \right] + \frac{V}{\rho} \frac{\partial V}{\partial R}) - \frac{2}{3} R_\theta (W \frac{\partial}{\partial R} \left[\frac{V}{\rho}. \right] + \frac{W}{\rho} \frac{\partial V}{\partial R})$$

$$+ n_r (W \frac{\partial}{\partial n} \left[\frac{W}{\rho}. \right] + \frac{W}{\rho} \frac{\partial W}{\partial n}) + n_\theta (V \frac{\partial}{\partial n} \left[\frac{W}{\rho}. \right] + \frac{V}{\rho} \frac{\partial W}{\partial n}) + n_z (U \frac{\partial}{\partial n} \left[\frac{W}{\rho}. \right]$$

$$+ \frac{U}{\rho} \frac{\partial W}{\partial n}) + \frac{4}{3} R_r (W \frac{\partial}{\partial R} \left[\frac{W}{\rho}. \right] + \frac{W}{\rho} \frac{\partial W}{\partial n}) + R_\theta (V \frac{\partial}{\partial R} \left[\frac{W}{\rho}. \right] + \frac{V}{\rho} \frac{\partial W}{\partial R})$$

$$+ R_z (U \frac{\partial}{\partial R} \left[\frac{W}{\rho}. \right] + \frac{U}{\rho} \frac{\partial W}{\partial R}) - \frac{1}{R} (\frac{2VW}{\rho} + \frac{4W}{3\rho}) \Big)$$

	P.S.	S.S.
BLADE BOUNDARY LAYER	W+	W+
SHED VORTICITY	W-	W+
TIP LEAKAGE	W+	W-
ANNULUS WALL SECON. FLOW	W+	W-
HUB WALL SECON. FLOW	W-	W+

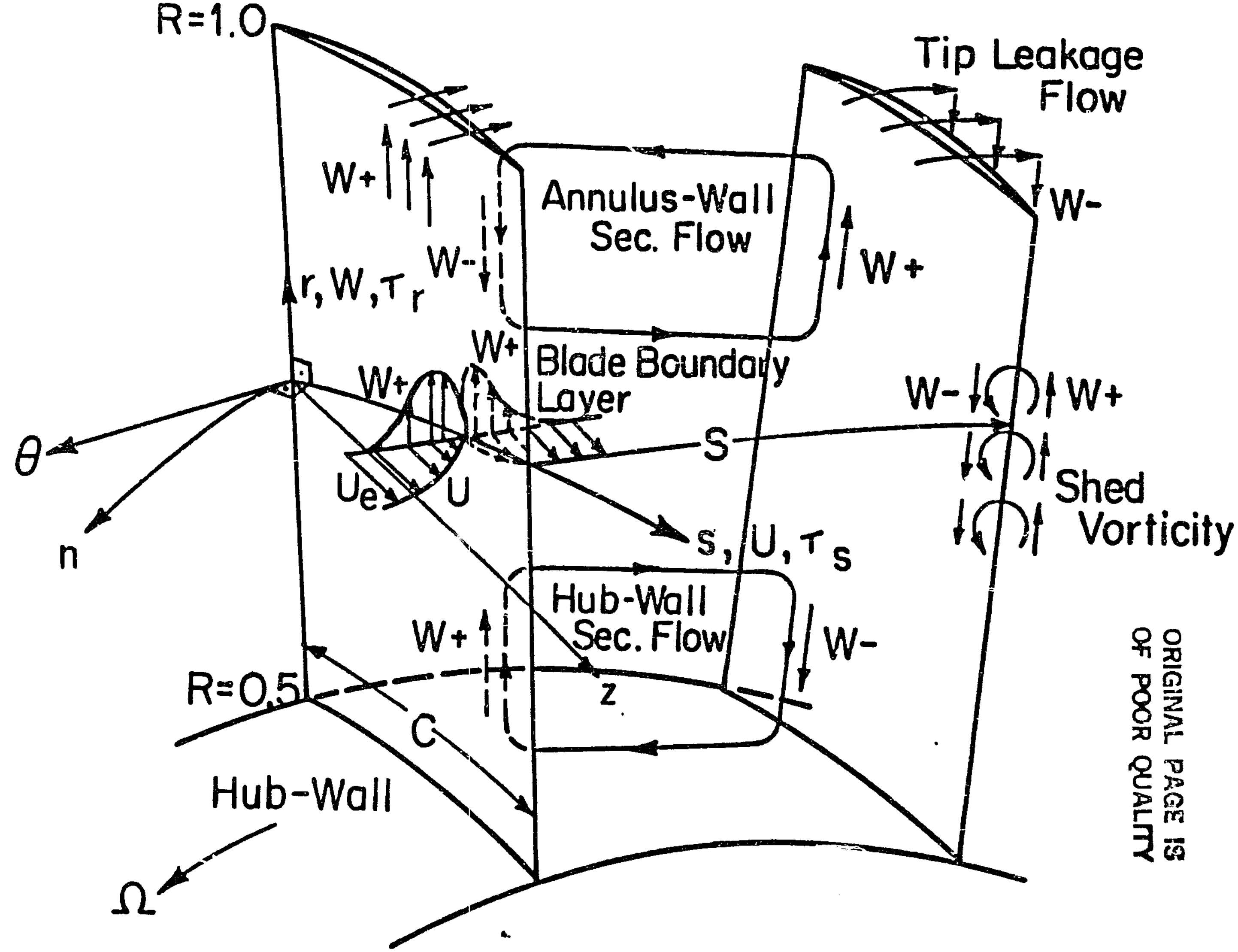

Fig. 1 Nature of Blade Boundary Layer and Notations Used

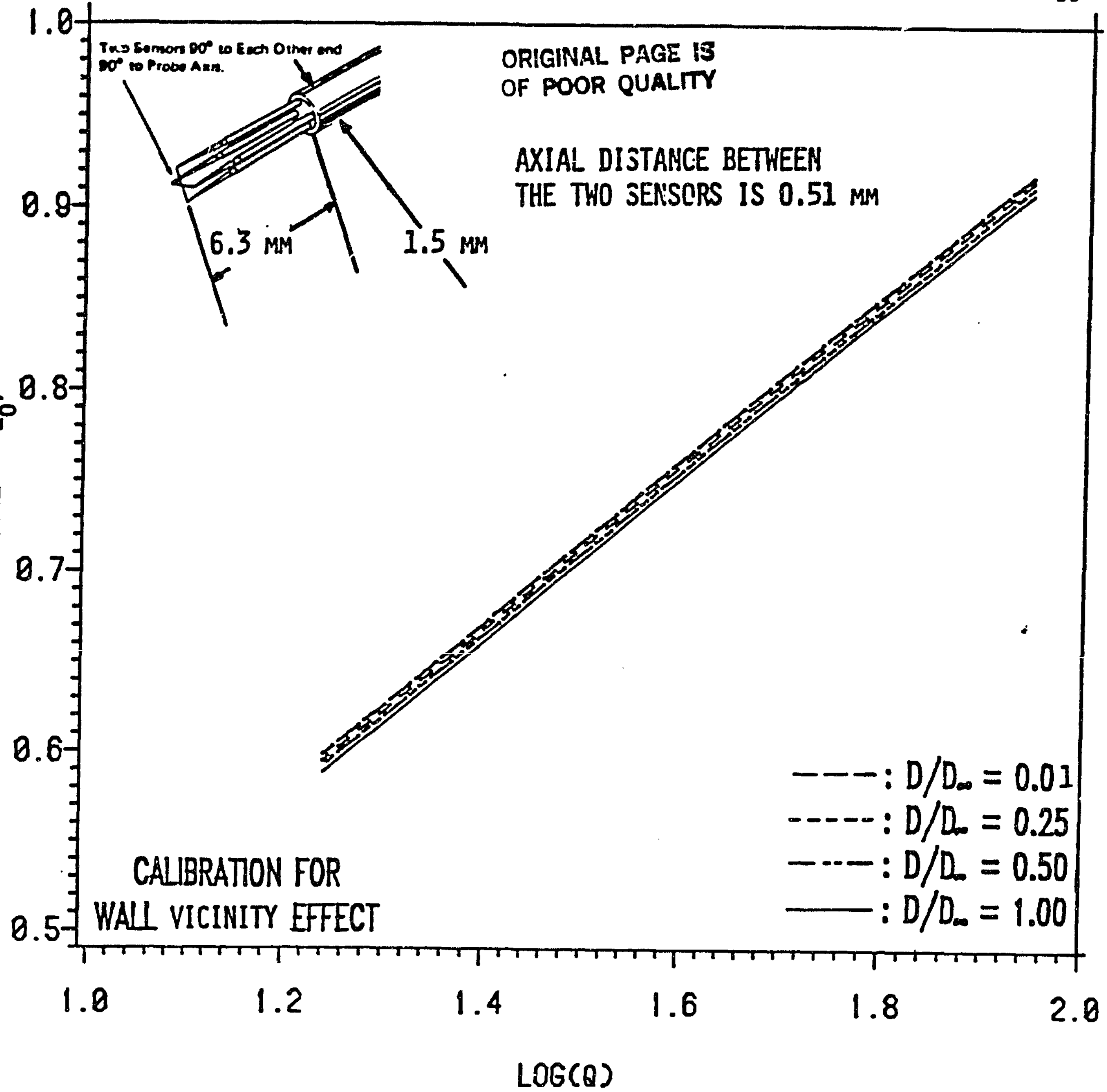

Fig. 2 Hot Wire Calibration Curves for Wall Vicinity Effect

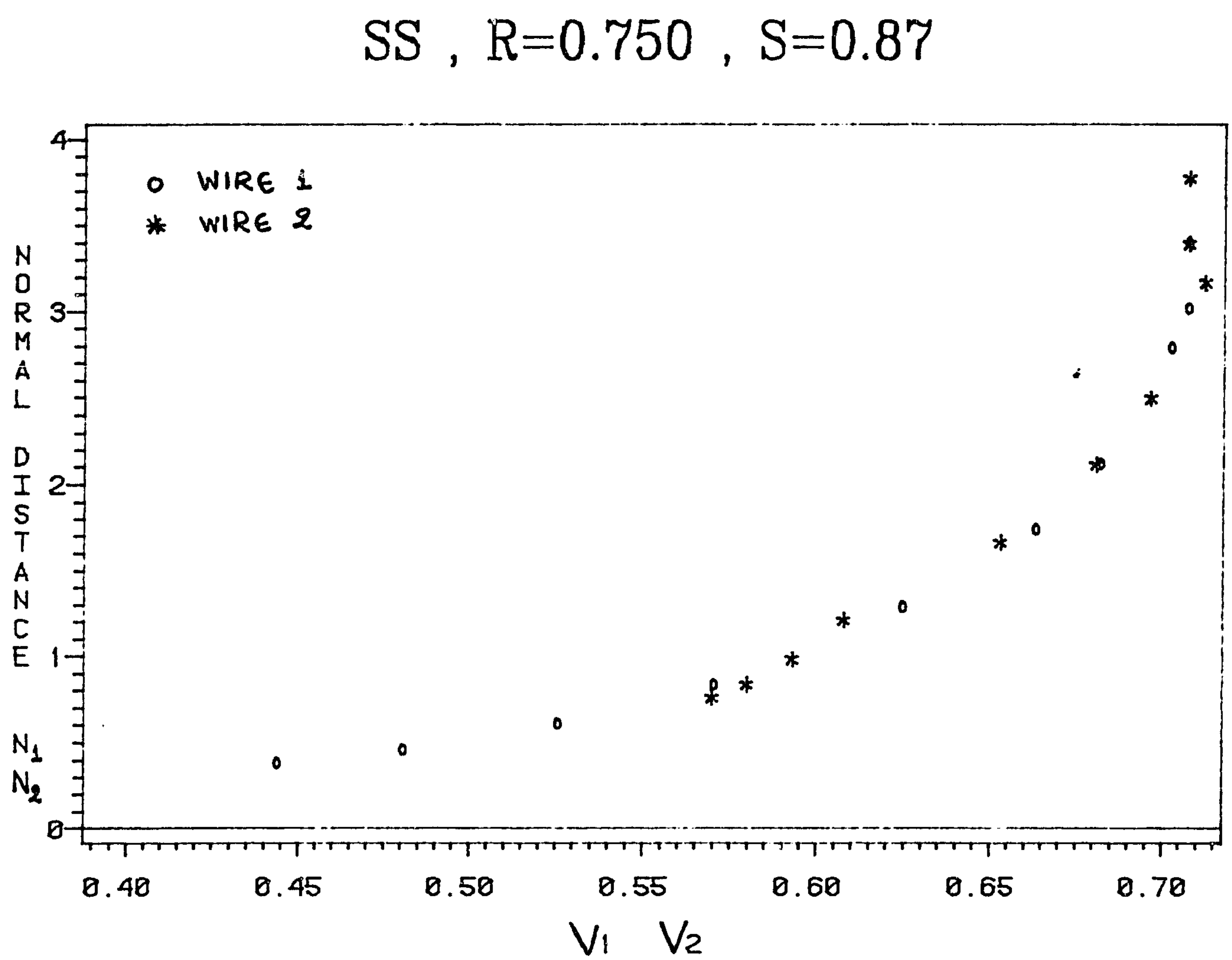

Fig. 3. Velocities V_1, V_2 felt by wires 1 and 2, respectively

ORIGINAL PAGE IS
OF POOR QUALITY

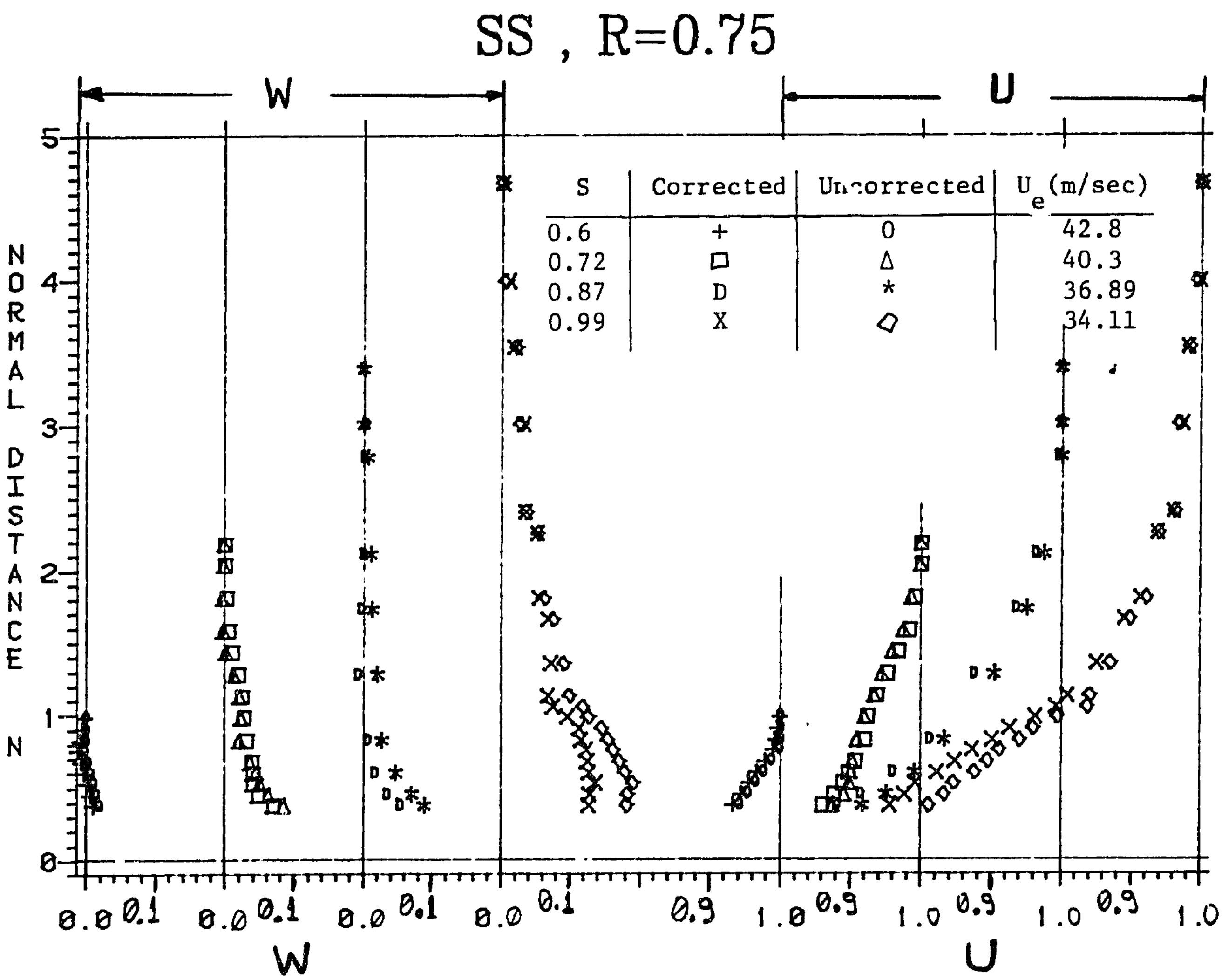

Fig. 4. Corrected and Uncorrected Velocity Profiles at R = 0.75 on the Suction Side

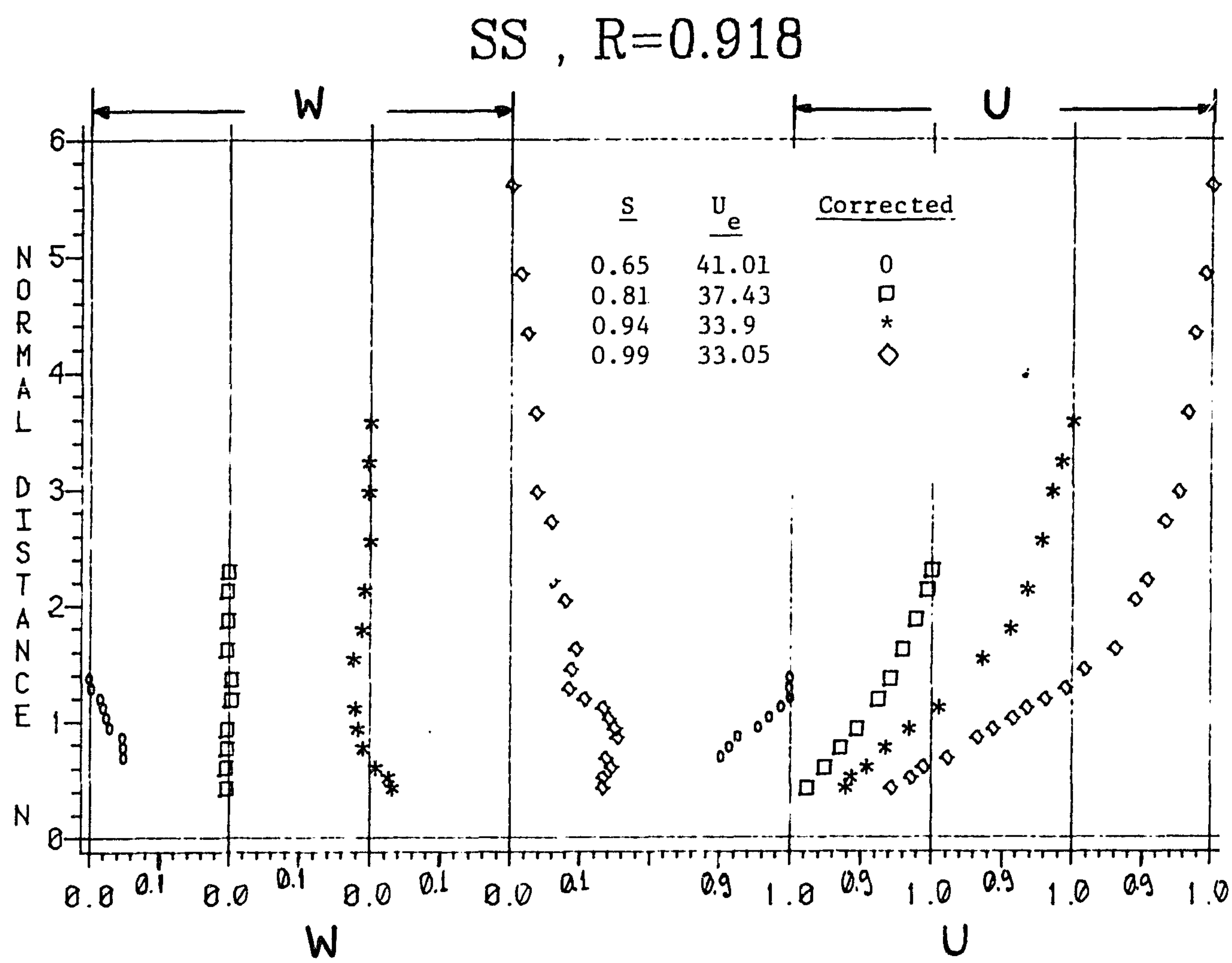

Fig. 5. Velocity Profiles at R = 0.918 on the Suction Side

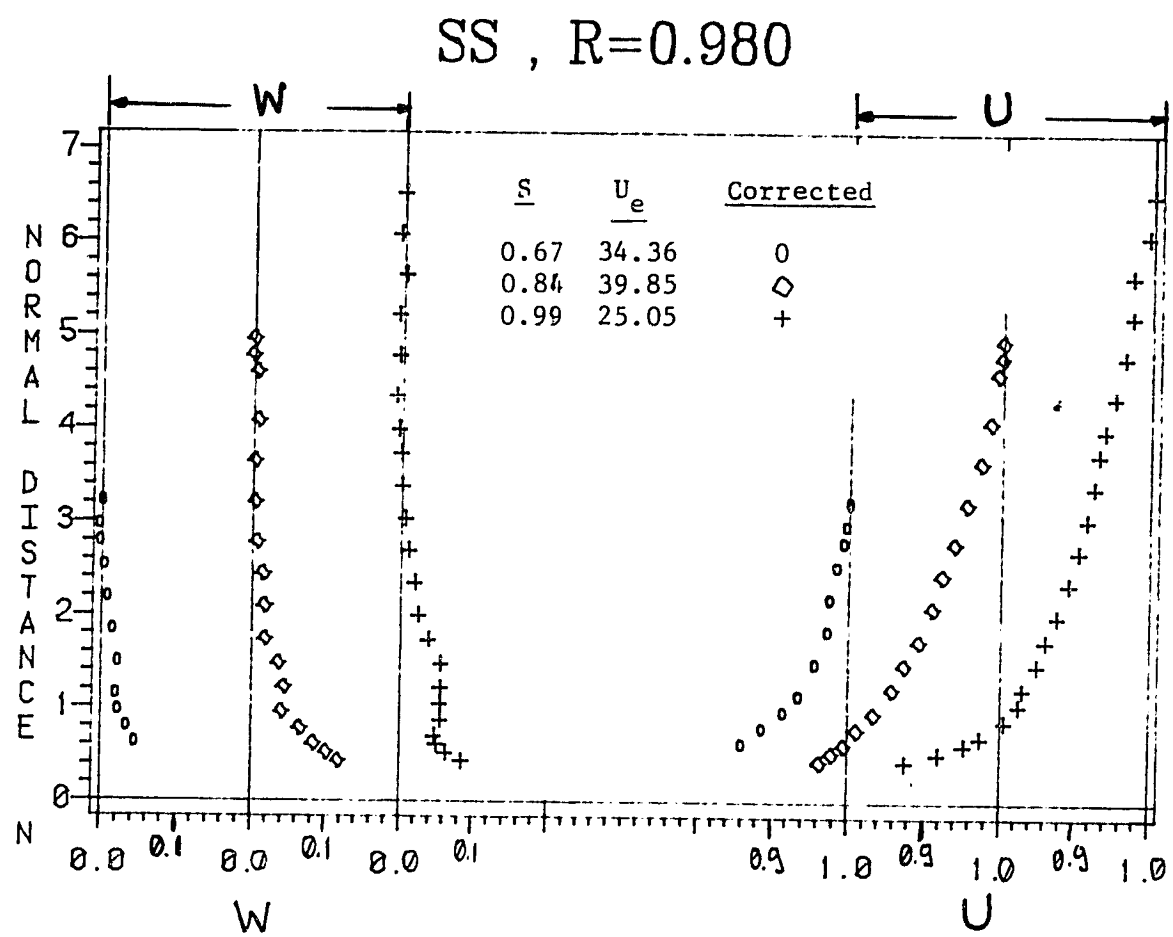

Fig. 6. Velocity Profiles at R = 0.98 on the Suction Side

ORIGINAL PAGE IS
OF POOR QUALITY

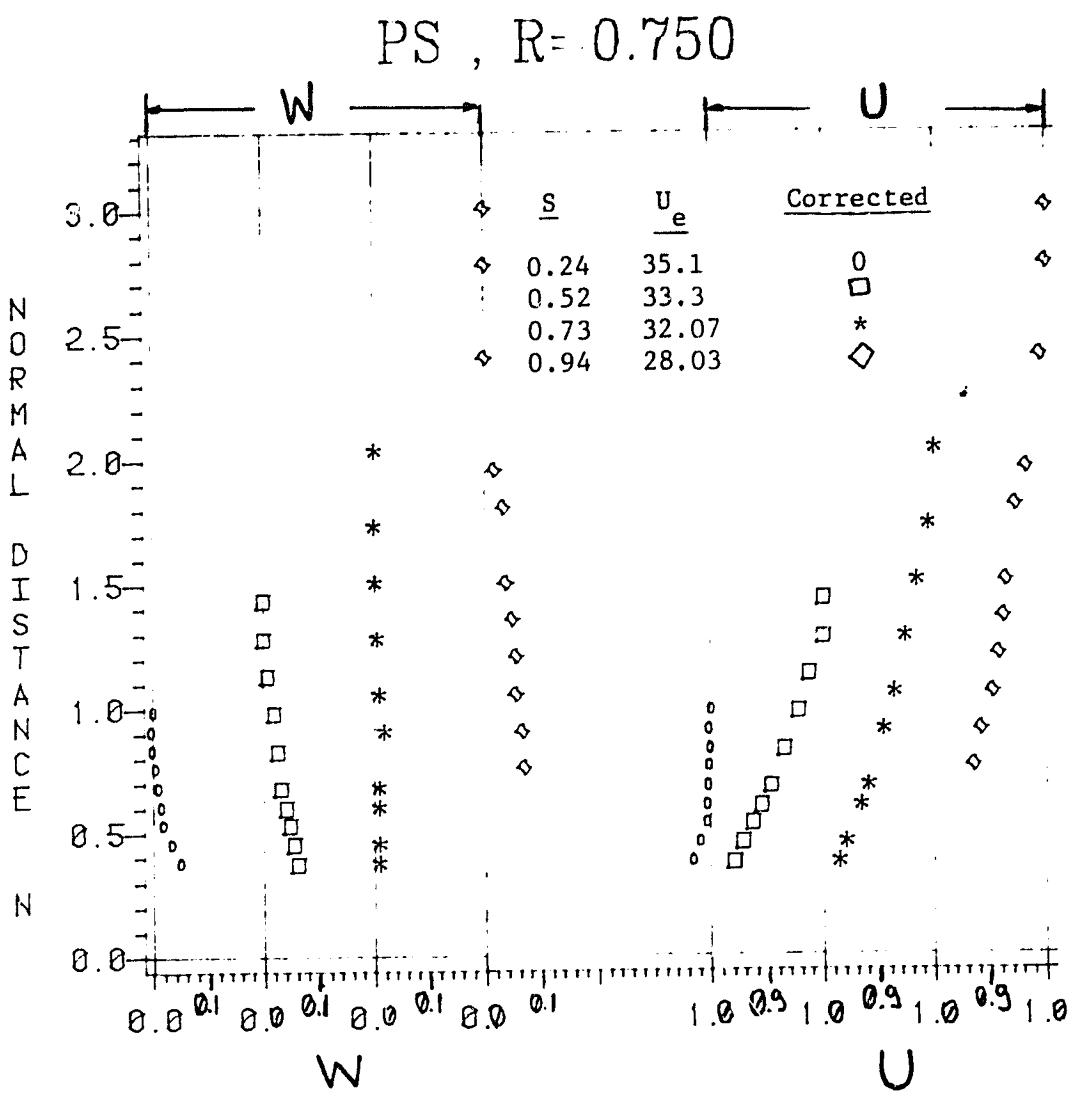

Fig. 7. Velocity Profiles at R = 0.75 on the Pressure Side

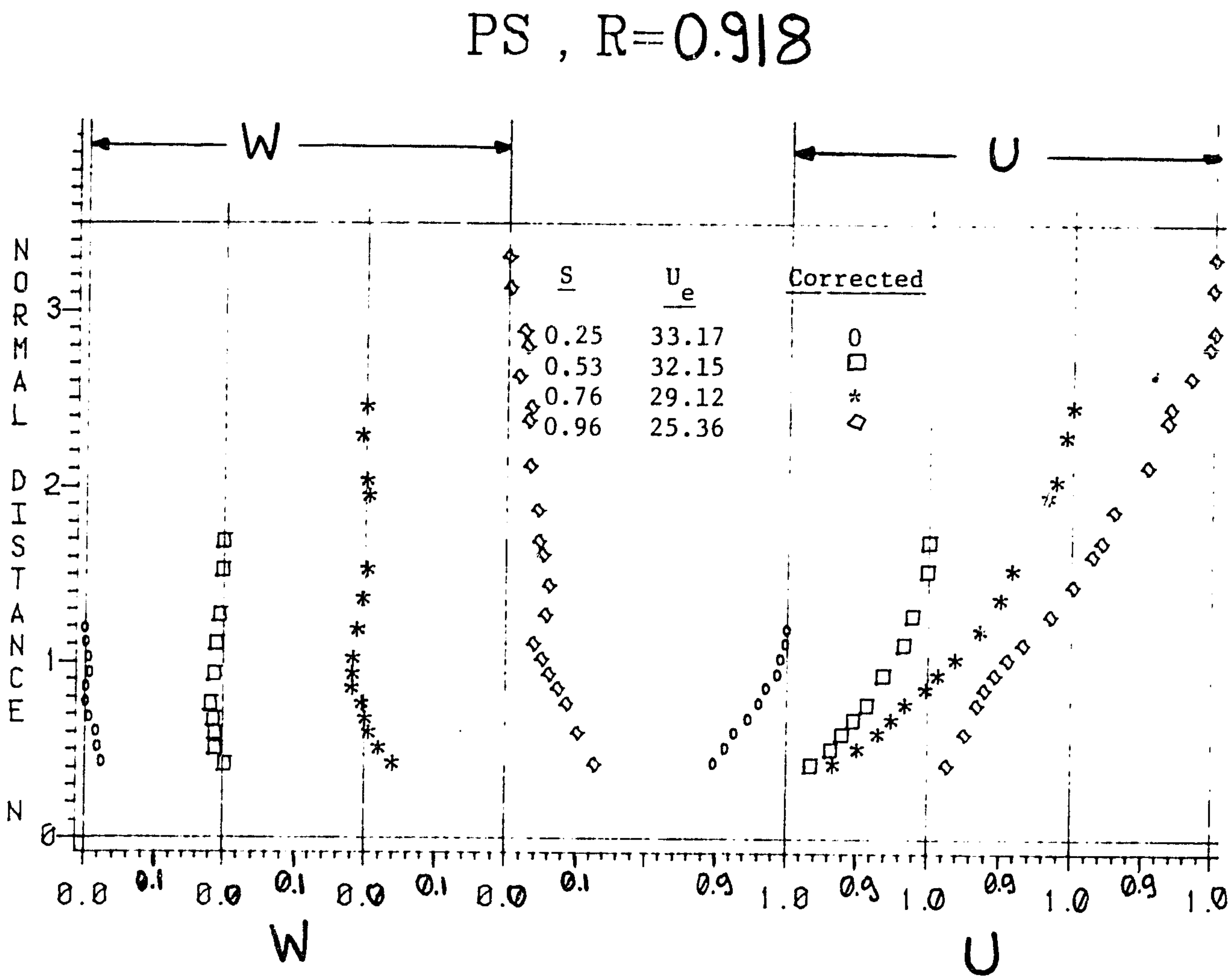

Fig. 8. Velocity Profiles at R = 0.918 on the Pressure Side

ORIGINAL PAGE IS
OF POOR QUALITY

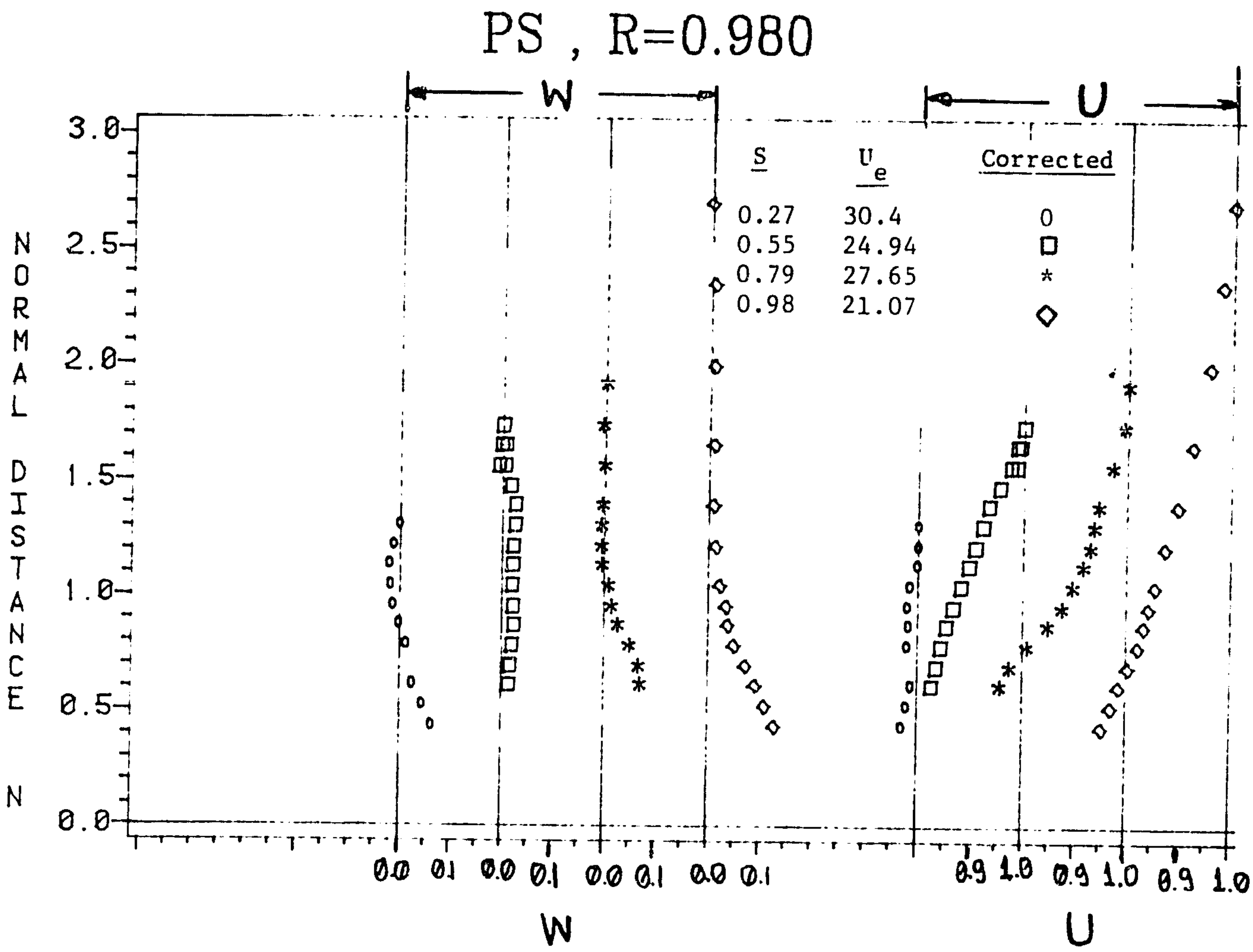

Fig. 9. Velocity Profiles at R = 0.98 on the Pressure Side

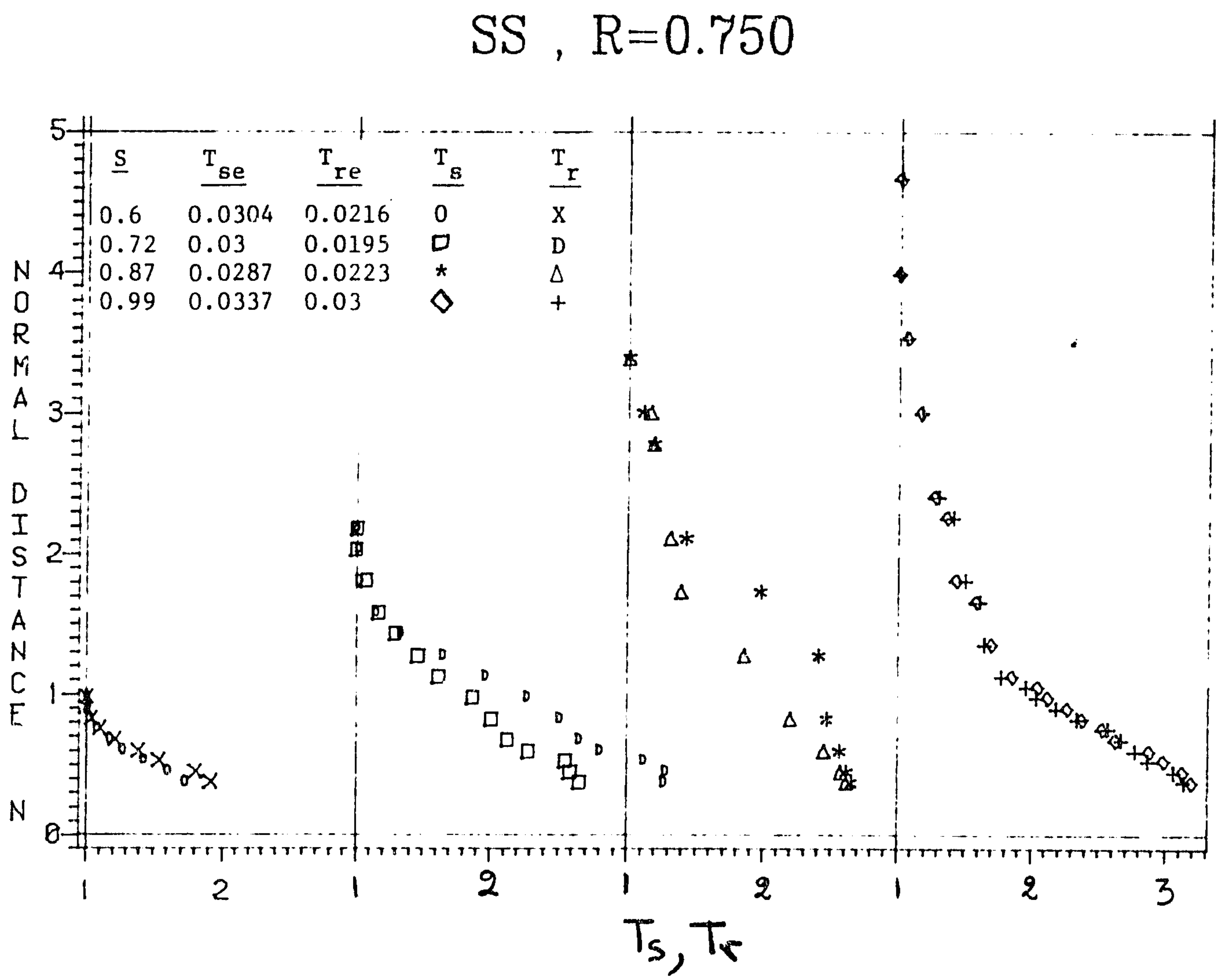

Fig. 10. Turbulent Intensity Profiles at R = 0.75 on the Suction Side

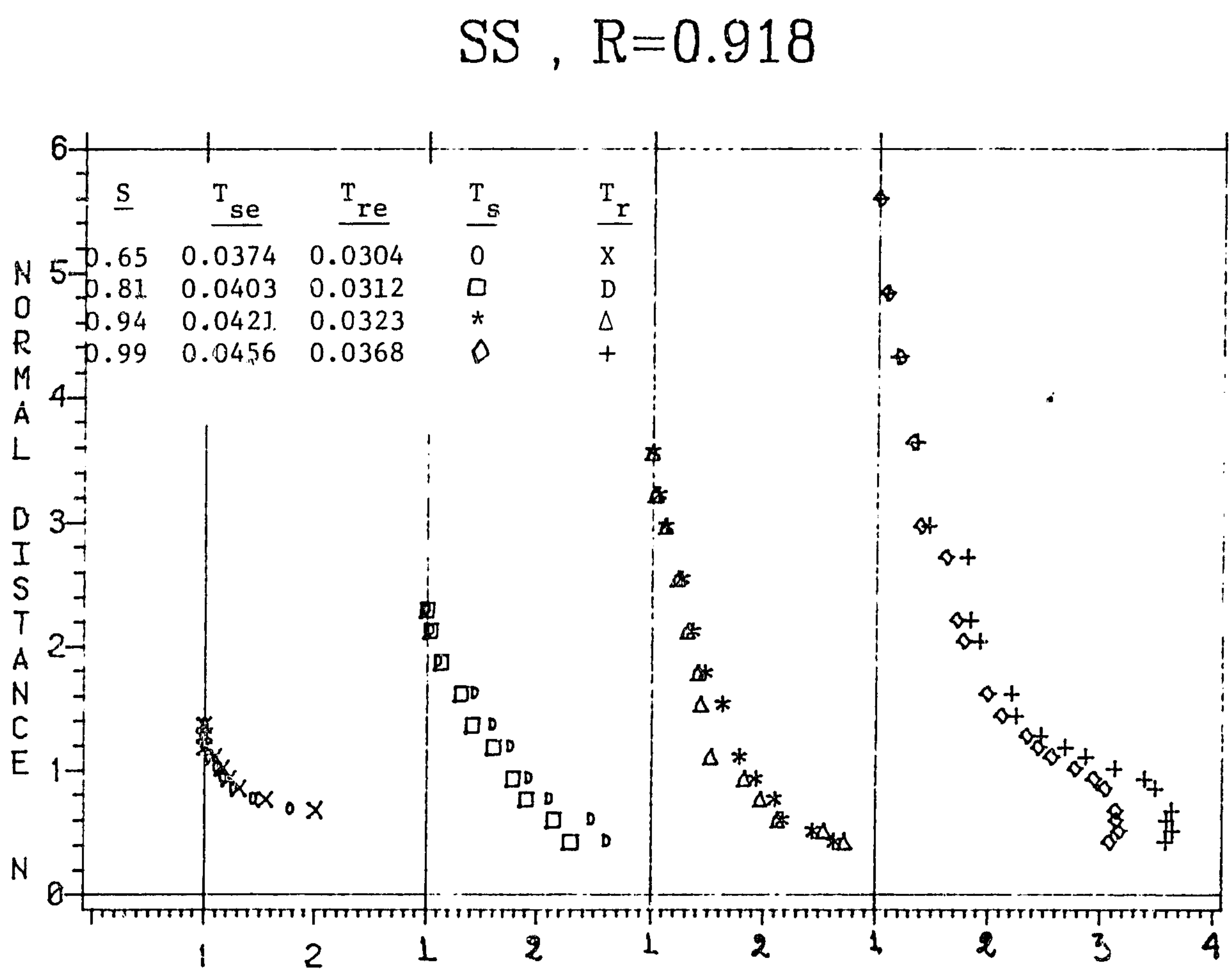

Fig. 11. Turbulent Intensity Profiles at R = 0.918 on the Suction Side

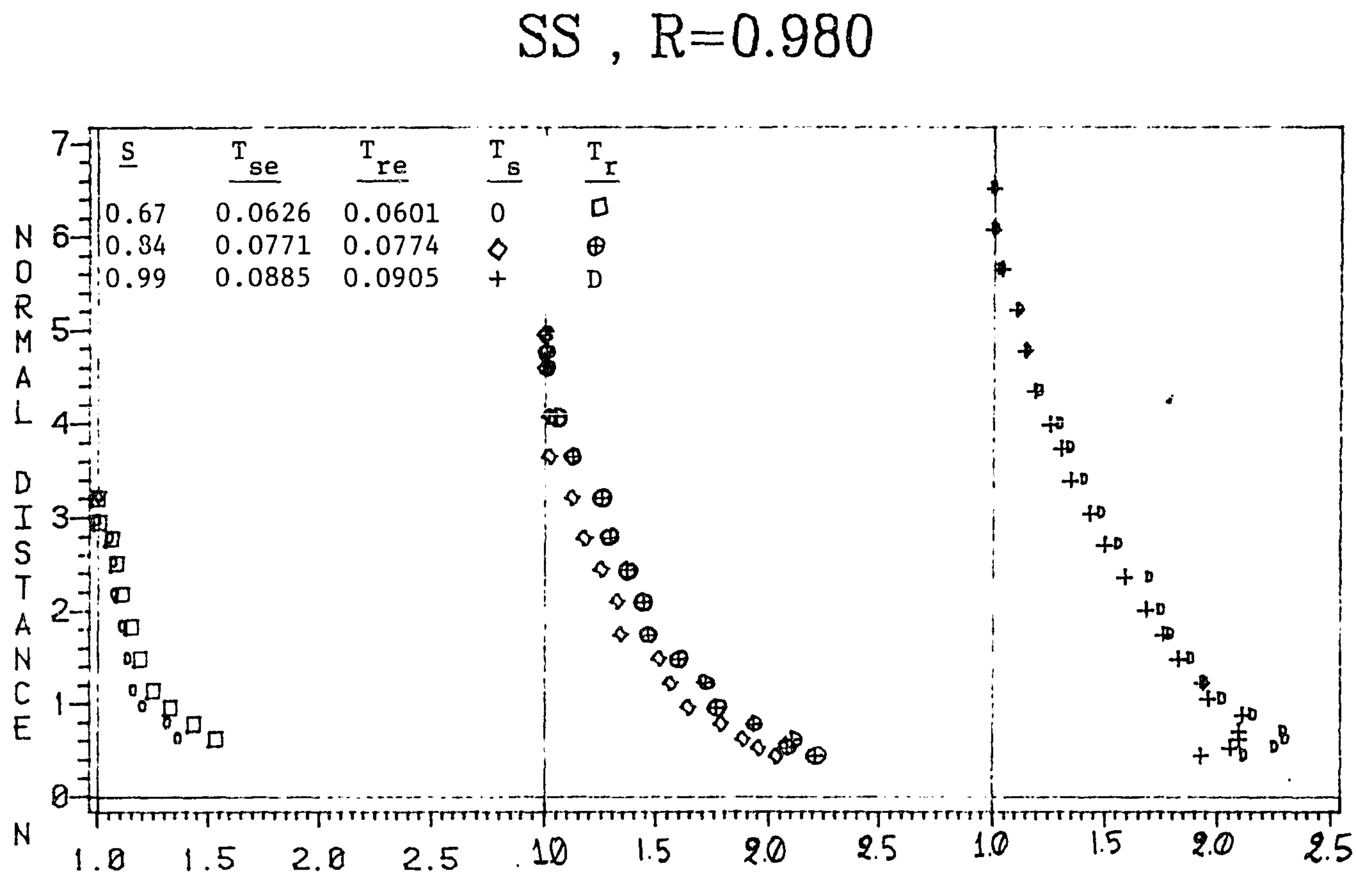

Fig. 12. Turbulent Intensity Profiles at R = 0.98 on the Suction Side

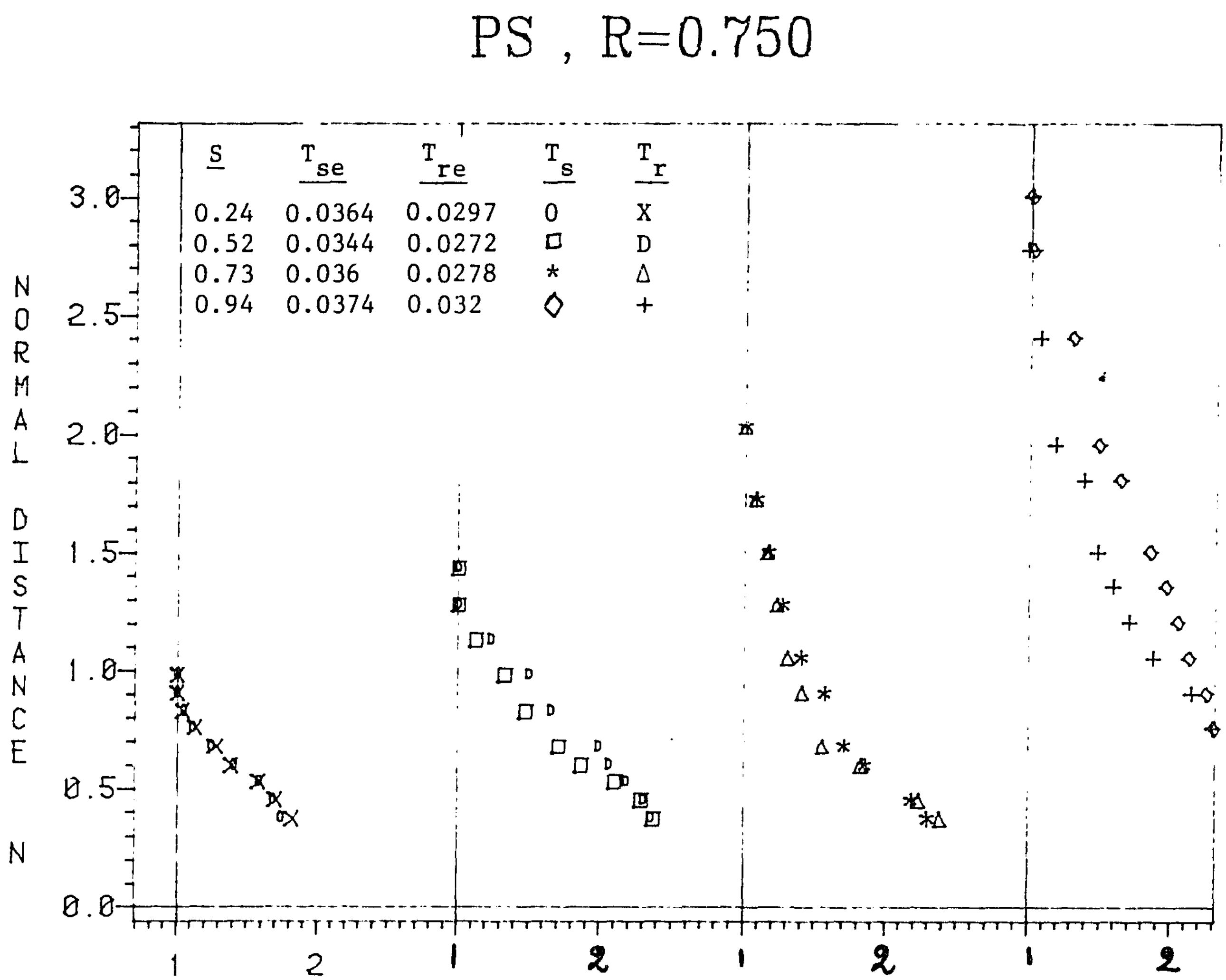

Fig. 13. Turbulent Intensity Profiles at R = 0.75 on the Pressure Side

ORIGINAL PAGE IS
OF POOR QUALITY

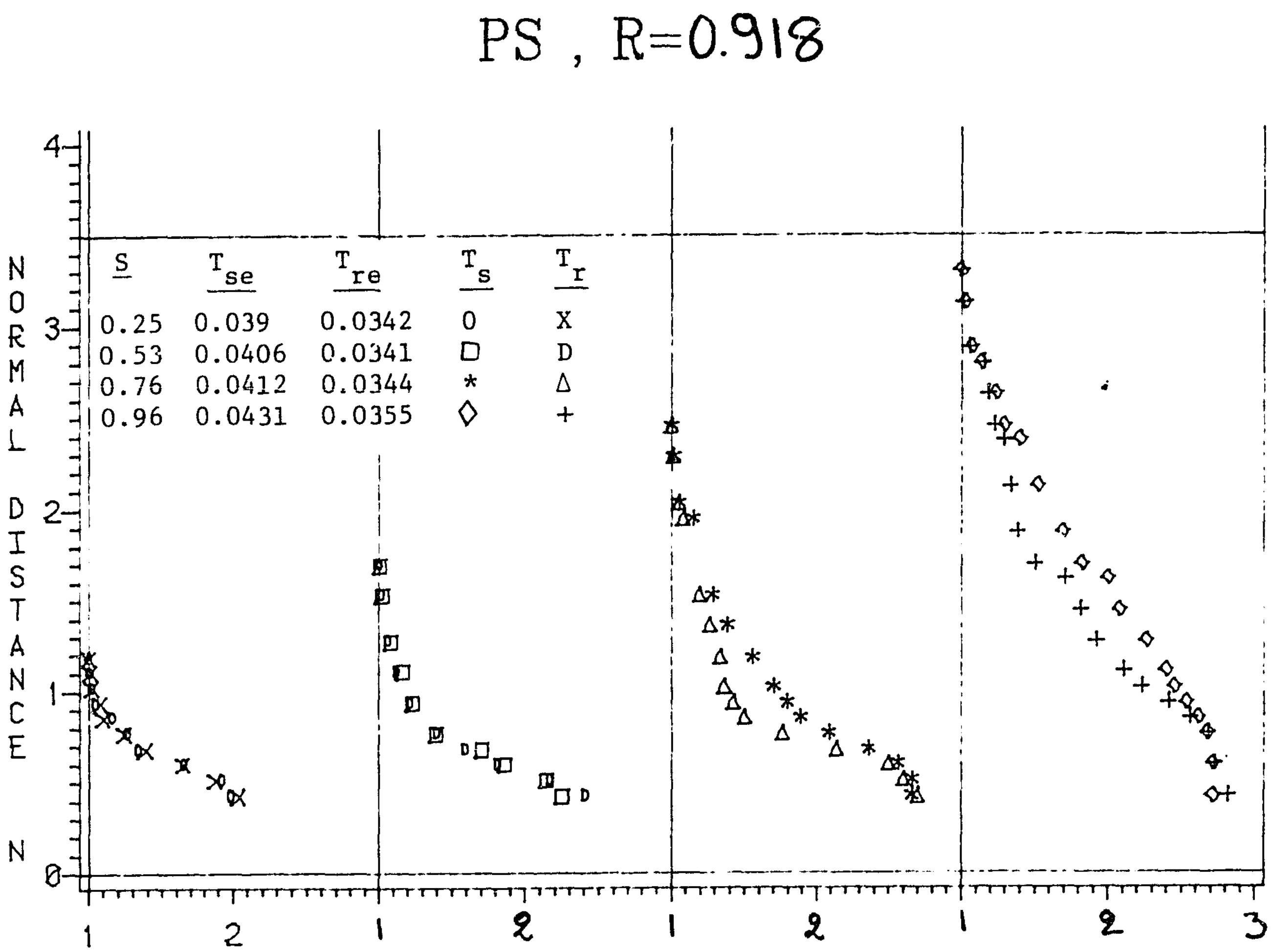

Fig. 14. Turbulent Intensity Profiles at R = 0.918 on the Pressure Side

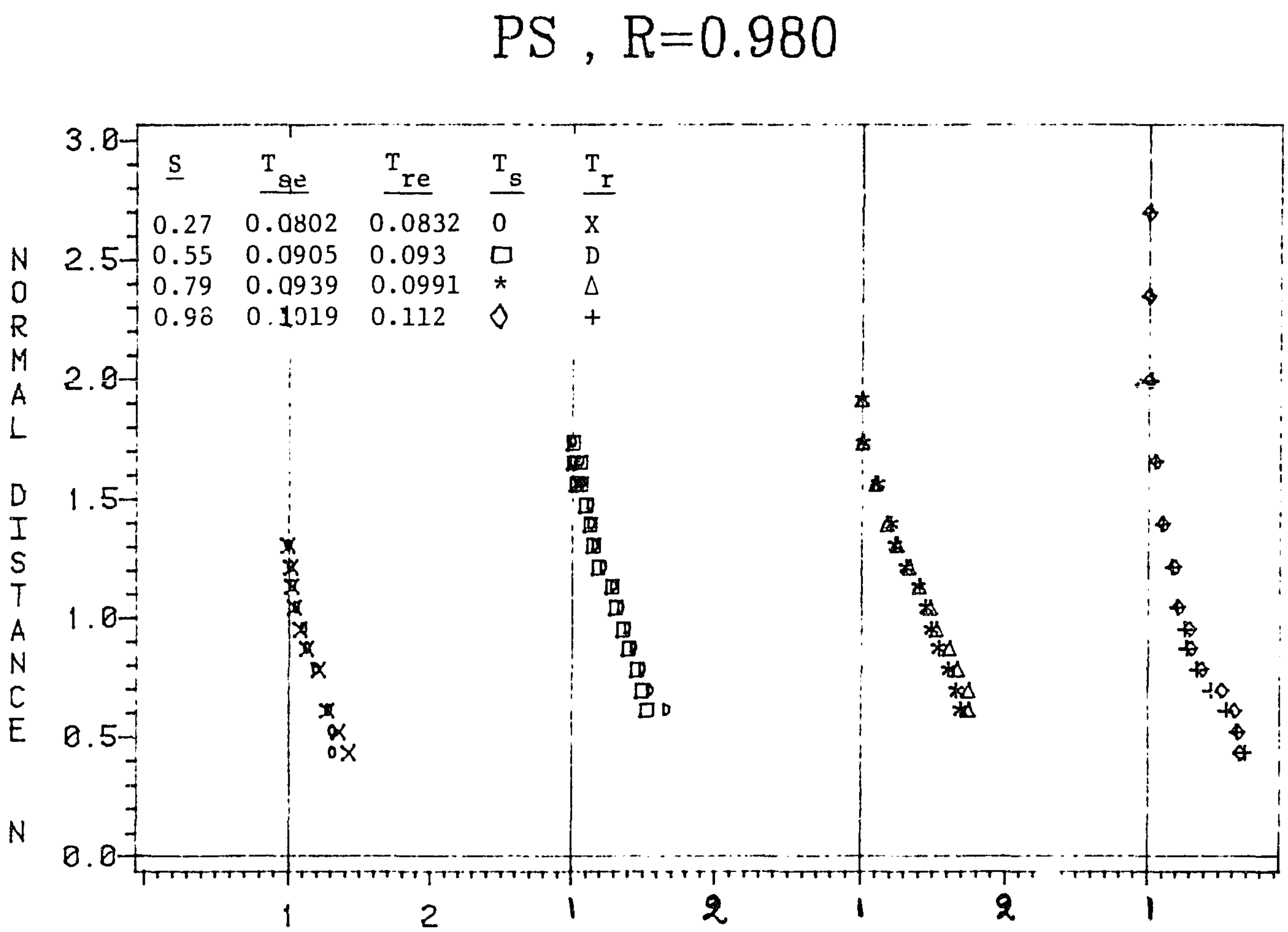

Fig. 15. Turbulent Intensity Profiles at R = 0.98 on the Pressure Side

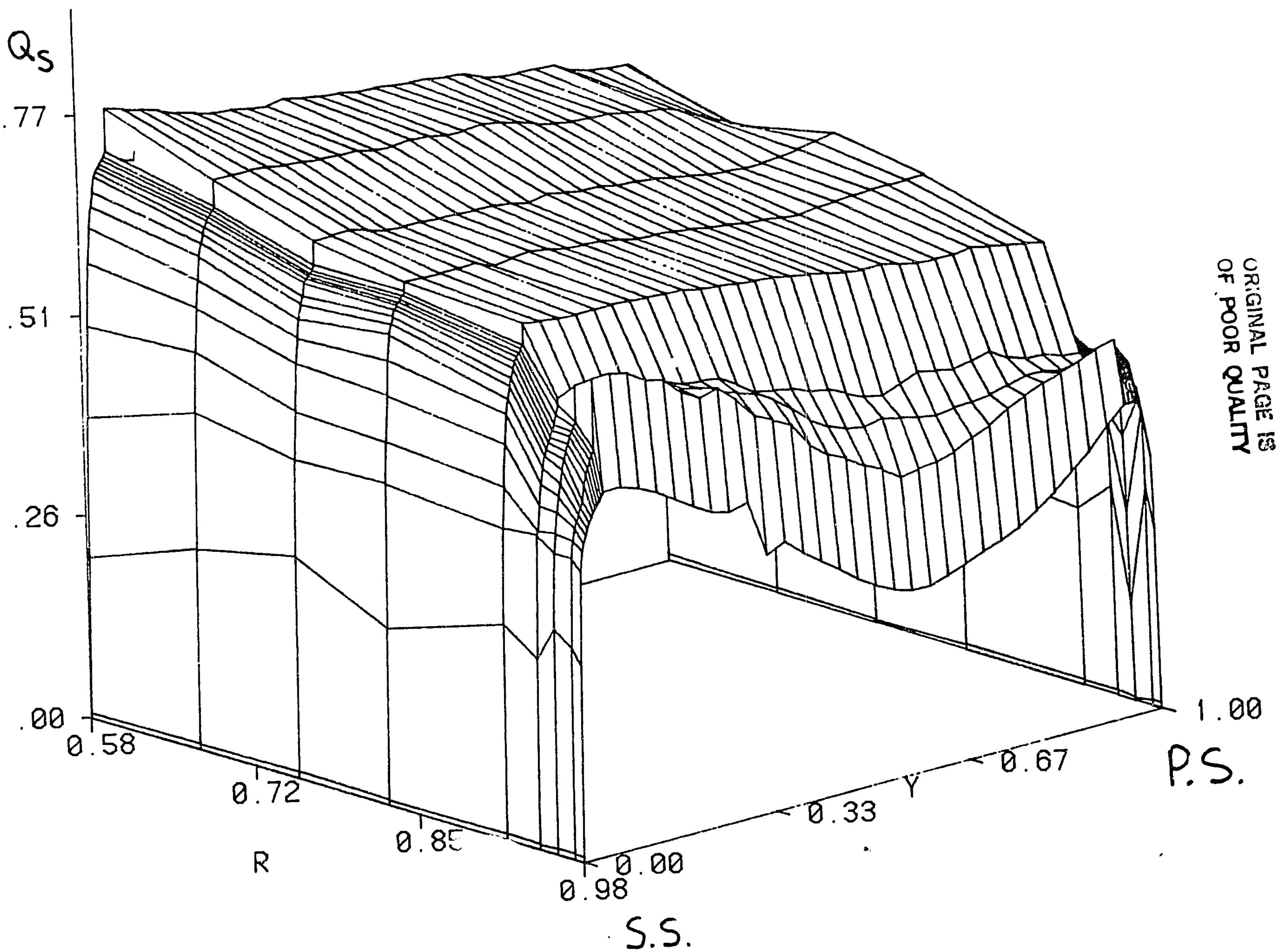

Fig. 16. Relative Streamwise Velocity at S = 0.979 (tip leakage data not included)

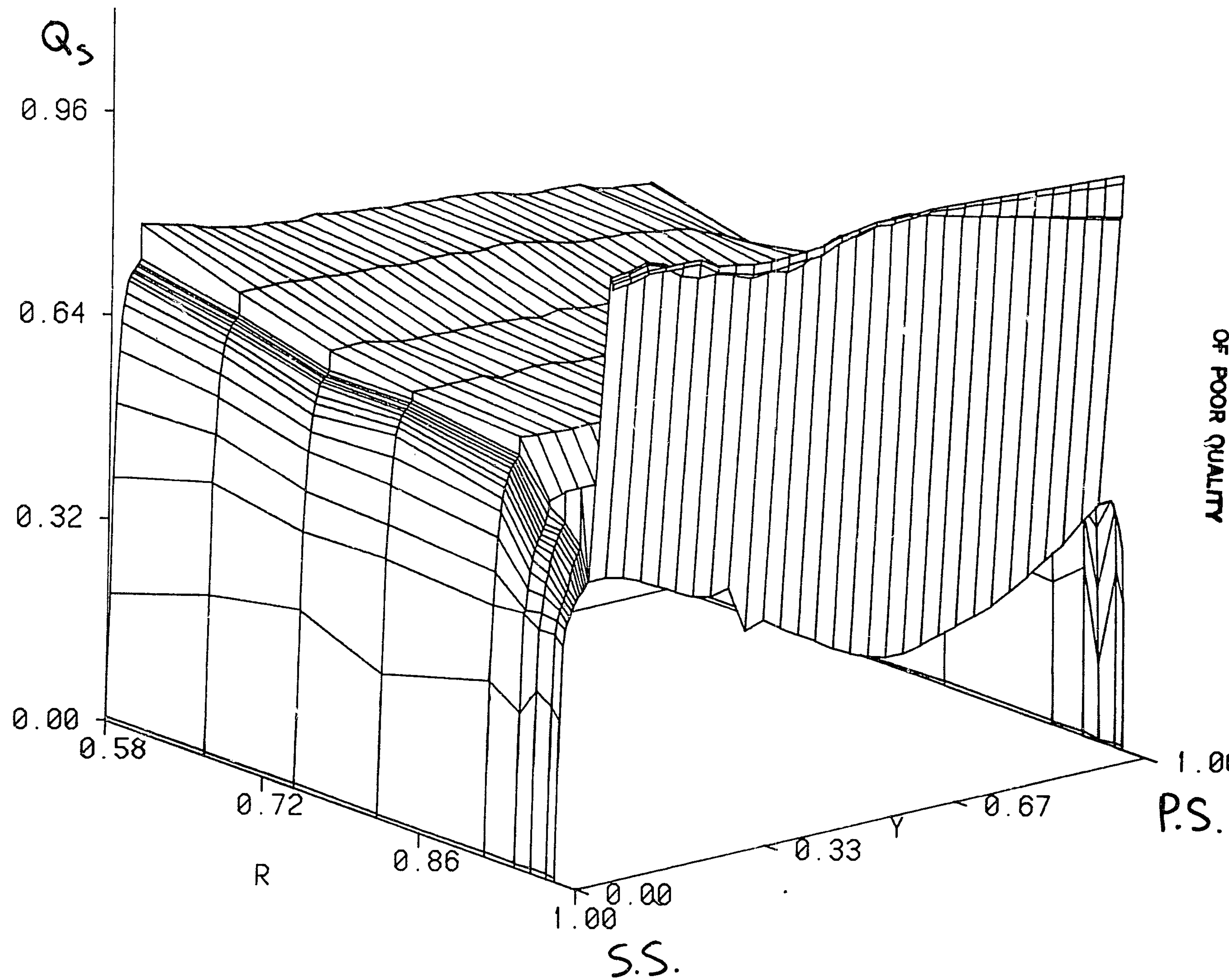

Fig. 17. Relative Streamwise Velocity at S = 0.979

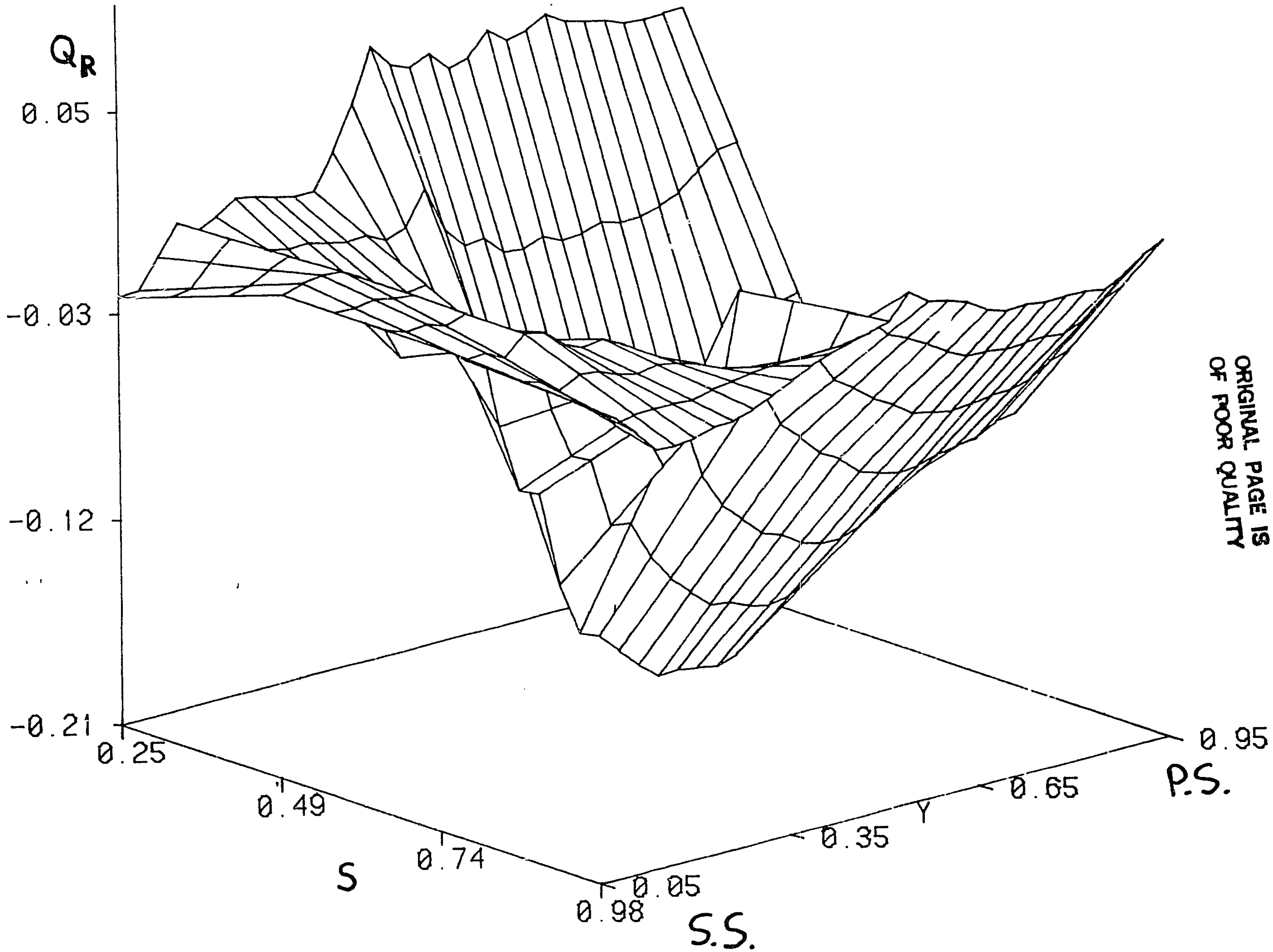

Fig. 18. Radial Velocity at R = 0.973

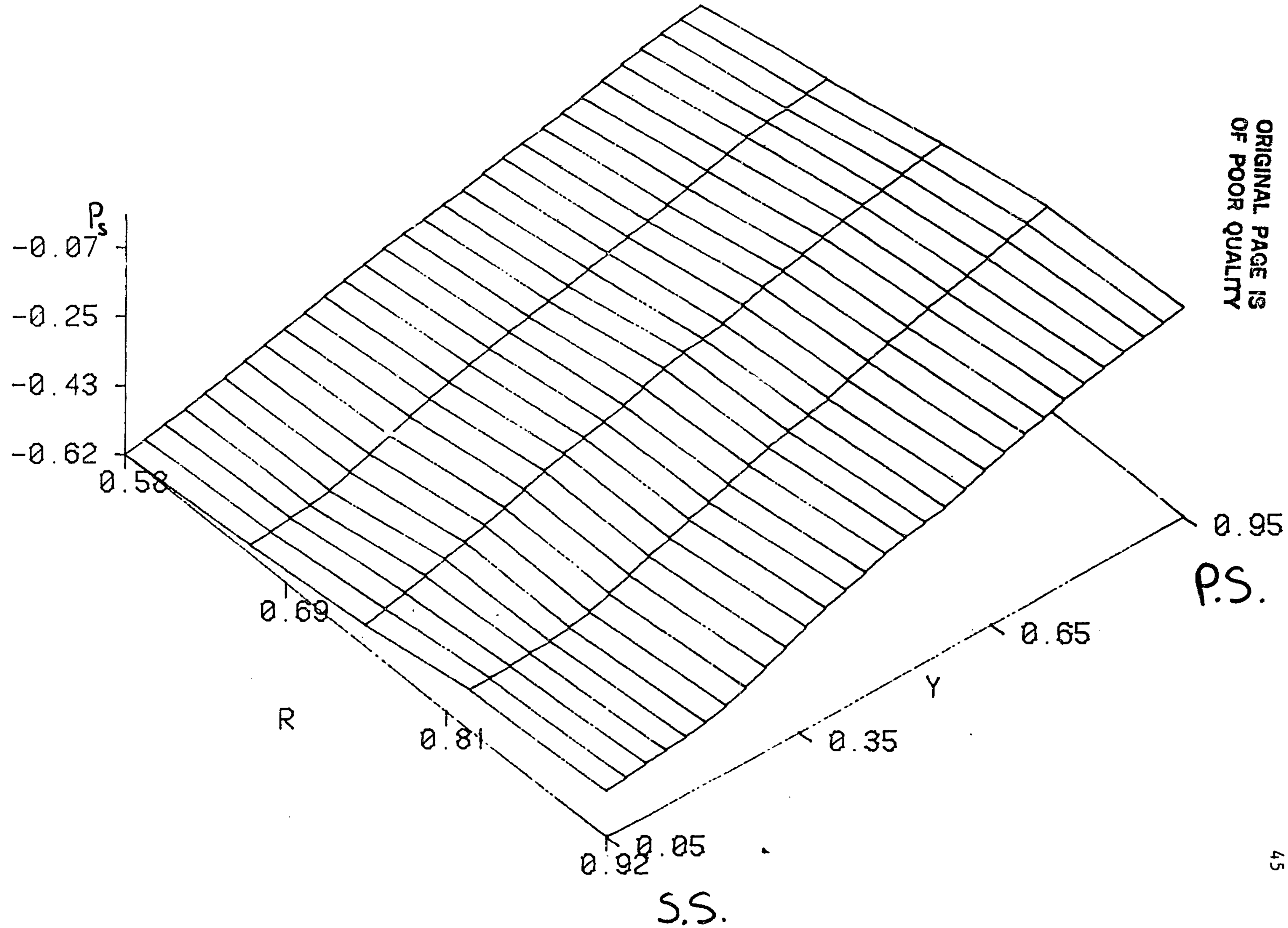

Fig. 19. Static Pressure at S = 0.25

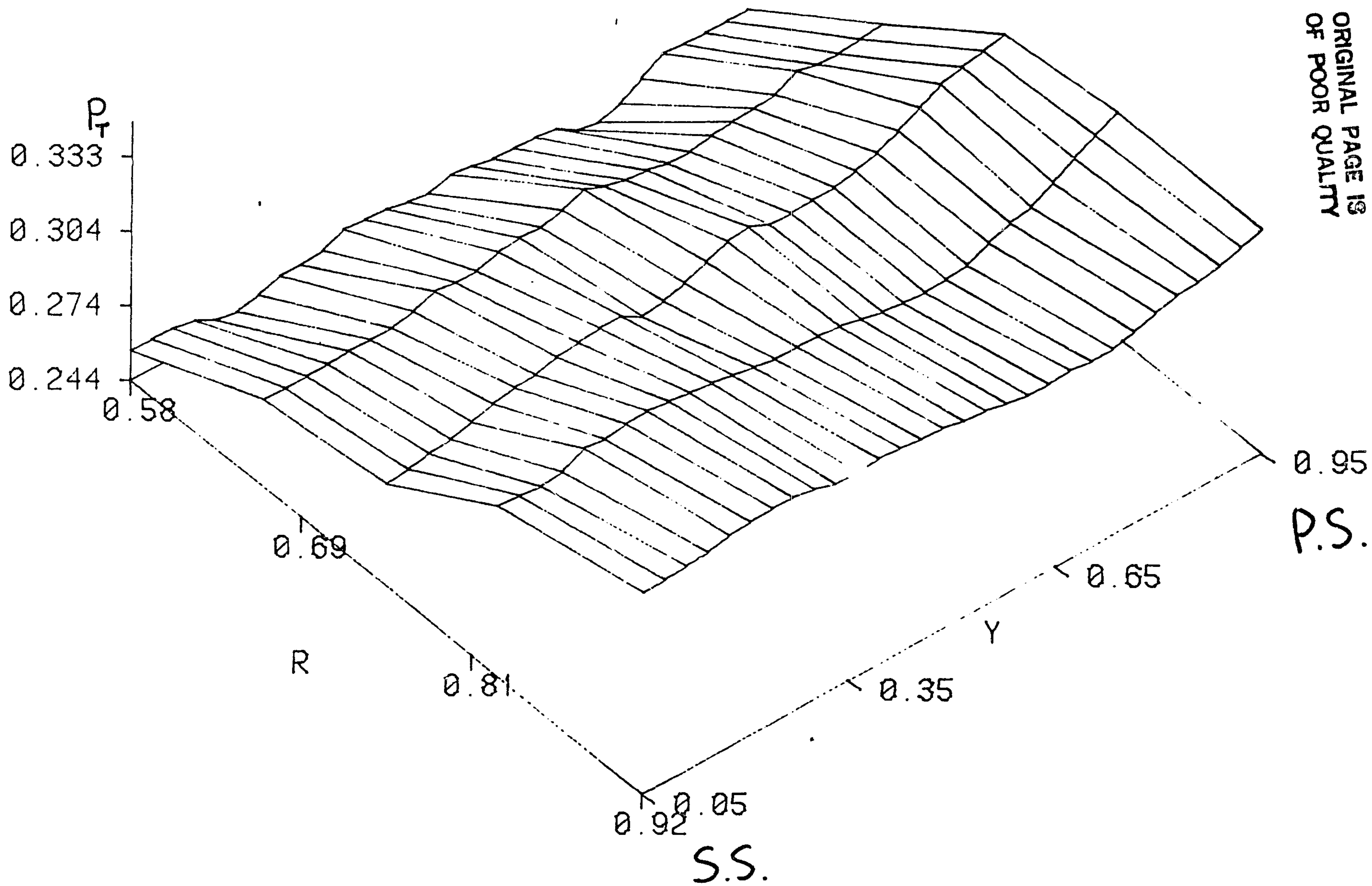

Fig. 20. Total Pressure at S = 0.979